

ORIGINAL RESEARCH

HNF4 α Acts as Upstream Functional Regulator of Intestinal Wnt3 and Paneth Cell FateChristine Jones,¹ Mariano Avino,² Véronique Giroux,¹ and Francois Boudreau¹¹Department of Immunology and Cell Biology, Université de Sherbrooke, Sherbrooke, Québec, Canada; and ²Department of Biochemistry and Functional Genomics, Université de Sherbrooke, Sherbrooke, Québec, Canada

SUMMARY

Enteroids lacking HNF4 α show changes in fate with reduction in Paneth and ISCs. HNF4 α acts as an upstream transcriptional regulator of *Wnt3*. HNF4 paralogs are not entirely redundant for intrinsic IEC functions when secluded from environmentally driven compensatory mechanisms.

BACKGROUND & AIMS: The intestinal epithelium intrinsically renews itself *ex vivo* via the proliferation of Lgr5⁺ intestinal stem cells, which is sustained by the establishment of an epithelial stem cell niche. Differentiated Paneth cells are the main source of epithelial-derived niche factor supplies and produce Wnt3 as an essential factor in supporting Lgr5⁺ stem cell activity in the absence of redundant mesenchymal Wnts. Maturation of Paneth cells depends on canonical Wnt signaling, but few transcriptional regulators have been identified to this end. The role of HNF4 α in intestinal epithelial cell differentiation is considered redundant with its paralog HNF4 γ . However, it is unclear whether HNF4 α alone controls intrinsic intestinal epithelial cell growth and fate in the absence of a mesenchymal niche.

METHODS: We used transcriptomic analyses to dissect the role of HNF4 α in the maintenance of jejunal epithelial culture when cultured *ex vivo* as enteroids in the presence or absence of compensatory mesenchymal cells.

RESULTS: HNF4 α plays a crucial role in supporting the growth and survival of jejunal enteroids. Transcriptomic analyses revealed an autonomous function of HNF4 α in *Wnt3* transcriptional regulation and Paneth cell differentiation. We showed that Wnt3a supplementation or co-culture with intestinal subepithelial mesenchymal cells reversed cell death and transcriptional changes caused by the deletion of *Hnf4a* in jejunal enteroids.

CONCLUSIONS: Our results support the intrinsic epithelial role of HNF4 α in regulating Paneth cell homeostasis and intestinal epithelium renewal in the absence of compensatory Wnt signaling. (*Cell Mol Gastroenterol Hepatol* 2023;15:593–612; <https://doi.org/10.1016/j.jcmgh.2022.11.010>)

Keywords: Enteroids; HNF4 α ; Paneth Cells; Wnt3.

The intestinal epithelium is an evolutionarily conserved biological system in which intestinal stem cells (ISCs), located at the bottom of the crypts of Lieberkühn, confer constant regenerative properties. ISC-

derived transit-amplifying crypt cells are continuously produced and differentiate into absorptive enterocytes and secretory cell lineages, including goblet, enteroendocrine, tuft, and Paneth cells.¹ Paneth cells constitute the epithelial niche but are dispensable *in vivo* for supporting ISC maintenance.^{2,3} In this context, intestinal mesenchymal cells can provide redundant niche signals to maintain epithelial ISC self-renewal, even in the absence of functional epithelial Wnt3 signaling.^{4–7} Recent studies have identified a variety of stromal cell lineages capable of generating redundant Wnt ligands that functionally contribute to the ISC niche under normal homeostasis.^{5,6,8–10} The plasticity of Paneth cells also serves as a mechanism to replenish ISCs during injury¹¹ and inflammation.¹² The inhibition of Notch and activation of Wnt signaling pathways are both required to support Paneth cell differentiation under these conditions.^{12,13} Transcription factor 4 (TCF4)¹⁴ and SOX9^{15,16} are the only transcription factors that have been reported to directly support Paneth cell differentiation.

HNF4 α , part of the nuclear receptor family, is expressed in the liver, pancreas, kidneys, epididymis, and gastrointestinal epithelium; more specifically, it is expressed in the foveolar, absorptive, goblet, and Paneth cells of the latter.¹⁷ HNF4 α acts as an epithelial morphogen^{18–20} and binds to villus differentiation genes,²¹ albeit without major consequences when conditionally deleted in the intestinal epithelium.^{18,21,22} Redundancy involving HNF4 α and HNF4 γ transcriptional functions supports these observations, whereas double deletion of these paralogs disrupts intestinal epithelial cell (IEC) differentiation in favor of an expansion of the proliferative zone.²³ This effect is possibly due to the prevention of the ability of crypt cells to differentiate, because both paralogs are required to support ISC renewal via the regulation of fatty acid β -oxidation genes.²⁴ Despite these observations, there is evidence that neither

Abbreviations used in this paper: ChIP-seq, chromatin immunoprecipitation sequencing; DMSO, dimethyl sulfoxide; EdU, 5-ethynyl-2-deoxyuridine; FDR, false discovery rate; GFP, green fluorescent protein; GSEA, gene set enrichment analysis; 4OHT, hydroxytamoxifen; IEC, intestinal epithelial cell; ISC, intestinal stem cell; PBS, phosphate-buffered saline; RNA-seq, RNA sequencing; RT-qPCR, quantitative real-time polymerase chain reaction; TCF4, transcription factor 4.



Most current article

© 2022 The Authors. Published by Elsevier Inc. on behalf of the AGA Institute. This is an open access article under the CC BY-NC-ND license (<http://creativecommons.org/licenses/by-nc-nd/4.0/>).

2352-345X

<https://doi.org/10.1016/j.jcmgh.2022.11.010>

paralog is entirely redundant for epithelial homeostasis during injury. HNF4 α alone is sufficient to sustain intestinal tumorigenesis in *APC^{min}* mice.²⁵ This implies an exclusive role for HNF4 α in ISC maintenance because *Lgr5*+ stem cells lacking *Apc* are the source of adenoma formation.²⁶ HNF4 α is also linked to inflammatory bowel diseases,^{27,28} whereas its sole conditional intestinal epithelial deletion in mice leads to features associated with these diseases.²⁹ These mutant mice are also defective in intestinal epithelial regeneration after irradiation.³⁰ In the same study, it was observed that organoids derived from the small intestine of HNF4 α mutant mice failed to propagate in vitro.³⁰ It thus appears that enteroids require HNF4 α for their maintenance in culture, in strong contrast to the in vivo situation. These important differences could be due to some redundancy from transcriptional functions of HNF4 family members that may operate differently in vivo and to the presence of pericryptal cell types in the intestine that may compensate for the loss of the ISC niche.

In this study, we dissected the intestinal epithelial functions of HNF4 α both in absence or presence of a compensatory mesenchymal niche. We found that jejunal enteroids lacking HNF4 α displayed changes in specific cell gene signatures with an alteration of Paneth cell function. This led to massive transcriptomic changes, followed by a loss of enteroid integrity. We also observed that HNF4 α acts as an upstream transcriptional regulator of *Wnt3*. Our data suggest that this regulatory loop is of functional importance, because *Wnt3a* or mesenchymal cell supplementation was able to significantly reduce the incidence of transcriptional changes and thus promote growth of HNF4 α -depleted jejunal enteroids in culture.

Results

Impact of *Hnf4a* Deletion on Enteroid Expansion in Culture

We isolated crypts from mutant *Villin-Cre; Hnf4a^{flox/flox}* (referred to as *Hnf4a^{ΔIEC}*) and control adult mice and monitored gene transcript expression for markers of ISCs, progenitors, and Paneth cells. ISC (*Lgr5*, *Ascl2*, *Olfm4*) and progenitor (*Ccnd1*, *Myc*) genes were not significantly modulated between the *Hnf4a^{ΔIEC}* mutant and control crypt cells (Figure 1A). Paneth-specific defensin genes (*Defa3*, *Defa5*, *Defa20*, *Defa21-20*) remained stable, whereas lysozyme (*Lyz*) and *Wnt3* transcript levels were significantly reduced in *Hnf4a^{ΔIEC}* mouse crypts (Figure 1A). WNT3 protein levels were also reduced under these conditions (Figure 1B). The mesenchymal source of WNTs compensates for Paneth cell deficiency in ISC maintenance.^{2,6,7} To examine the epithelial-intrinsic impact of *Hnf4a* deletion in intestinal crypts, we cultured and expanded isolated jejunal crypts into enteroids. Although both control and *Hnf4a^{ΔIEC}* mutant crypts rapidly formed enteroids with a flat epithelial layer, *Hnf4a^{ΔIEC}* mutant enteroids began degenerating between days 3 and 4 immediately after entering the culture (Figure 2A). This observation is reminiscent of that of enteroids lacking *Wnt3*, Paneth cells, or HNF4 α .^{2,7,30} We then generated *Villin-Cre^{ERT2}; Hnf4a^{flox/flox}* (referred to as

Hnf4a^{ΔIEC-ind}) mice allowing tamoxifen-inducible *Hnf4a* deletion under enteroid culture conditions. As observed in *Hnf4a^{ΔIEC}* mutant jejunal enteroids, hydroxytamoxifen (4OHT)-treated *Hnf4a^{ΔIEC-ind}* jejunal enteroids began to degenerate after 4 days of deletion, in contrast to vehicle-treated *Hnf4a^{ΔIEC-ind}* jejunal enteroids, which formed robust and typical crypt-budding structures (Figure 2B). The *Hnf4a^{ΔIEC-ind}* jejunal enteroids displayed reduced expression of both *Hnf4a* and *Wnt3* gene transcripts after 4OHT supplementation (Figure 2C and D). The degenerative phenotype of 4OHT-treated *Hnf4a^{ΔIEC-ind}* jejunal enteroids coincided with a reduction in 5-ethynyl-2-deoxyuridine (EdU) levels in proliferative cells within the crypt domains (Figure 2E), an effect that was statistically significant ($P < .05$) when quantified by flow cytometry (Figure 2F). Overall, these observations indicated that the loss of HNF4 α expression in crypt cells did not impair crypt homeostasis in vivo but severely affected jejunal enteroid expansion and maturation in culture.

Impact of *Hnf4a* Deletion on the Transcriptome and Cell Fate of Jejunal Enteroids

To further characterize the nature of the molecular changes that occur upon the loss of HNF4 α in jejunal enteroids, transcriptomic analysis was performed after days 2 and 4 in deleted *Hnf4a^{ΔIEC-ind}* jejunal enteroids immediately before the enteroids started to degenerate. RNA sequencing (RNA-seq) identified 4,356 gene transcripts that were significantly altered (false discovery rate [FDR] < 0.05) after 2 days of *Hnf4a* deletion, of which 608 gene transcripts were modulated by more than 2-fold (Supplementary Table 1). Gene ontology analysis of these 608 gene transcripts identified biological processes, such as acute inflammatory response, plasma membrane and extracellular matrix organization, regulation of cell migration, and lipid metabolic processes, as significant functional annotations (Figure 3A). Similarly, RNA-seq performed 4 days after *Hnf4a* deletion identified 4,769 gene transcripts that were significantly altered (FDR < 0.05), of which 738 gene transcripts were modulated more than 2-fold (Supplementary Table 2). Gene ontology analysis of these 738 genes also identified functions similar to those listed above (Figure 3B). These observations were unexpected, because deletion of *Hnf4a* in the murine small intestine in vivo has been reported to poorly influence the transcriptome, while requiring simultaneous deletion of its paralog *Hnf4g* for significant impacts to be seen on intestinal epithelial transcription and homeostasis.²³⁻²⁵ Closer inspection of *Hnf4g* expression after *Hnf4a* deletion in jejunal enteroids revealed 1.2-fold (after 2 days of deletion; Supplementary Table 1) and 1.4-fold increase (after 4 days of deletion; Supplementary Table 2) in levels of this gene transcript, negating the suggestion of the occurrence of a phenotype reminiscent of double *Hnf4a* and *Hnf4g* knockouts. These observations indicate that the loss of HNF4 α in jejunal enteroids that are deprived of a natural mesenchymal niche significantly impacts the transcriptome as opposed to the in vivo environment.

Because intestinal crypt lineage determination is strongly dependent on lineage-restricted transcription factors,^{31,32} we

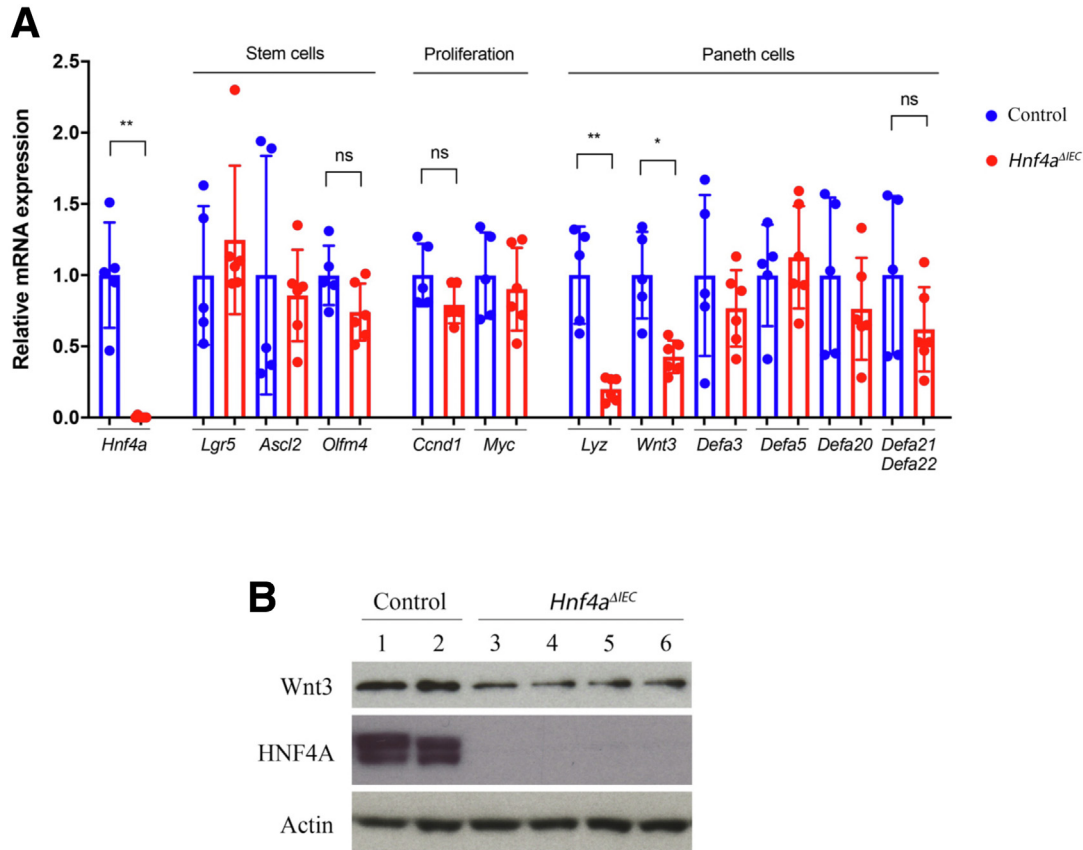
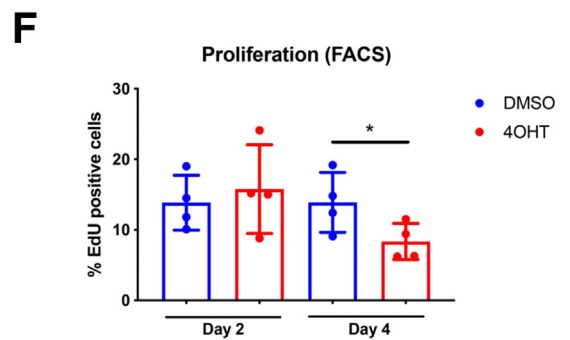
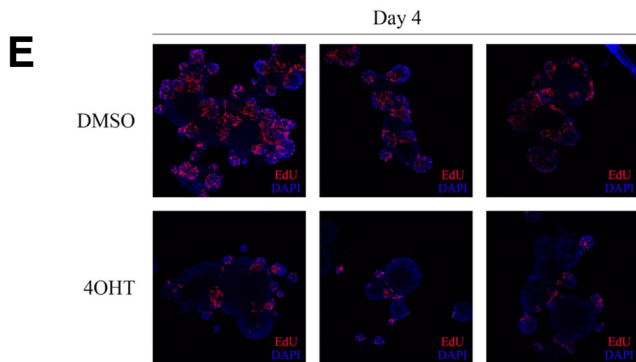
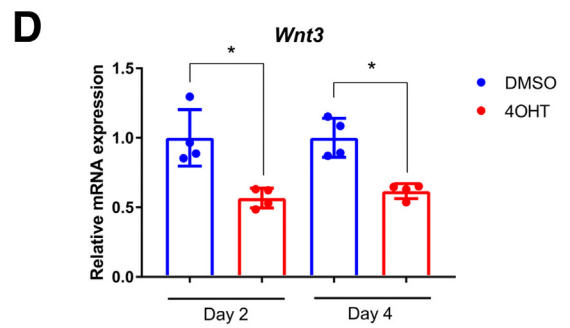
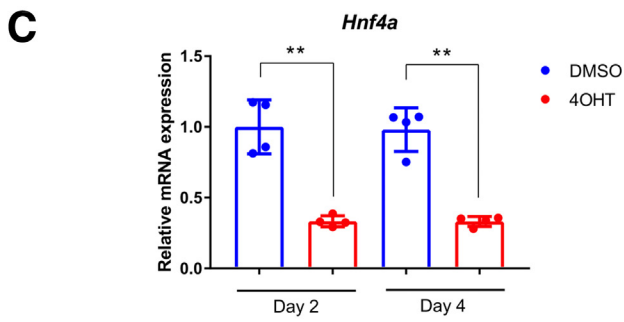
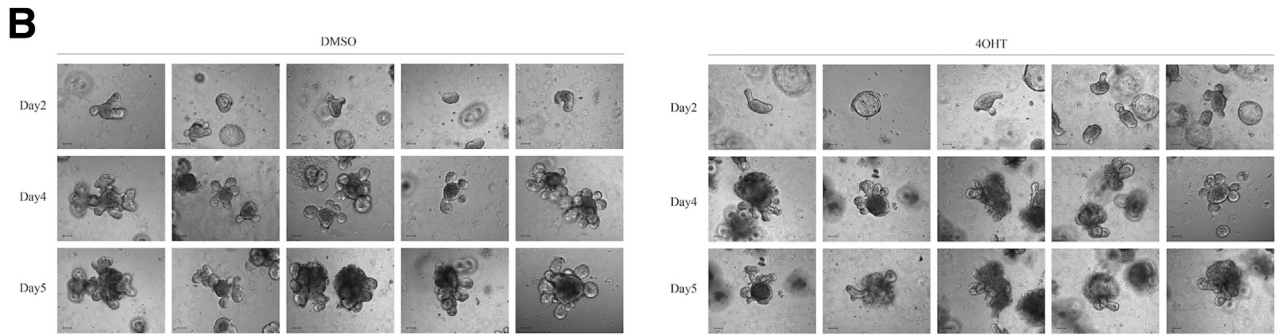
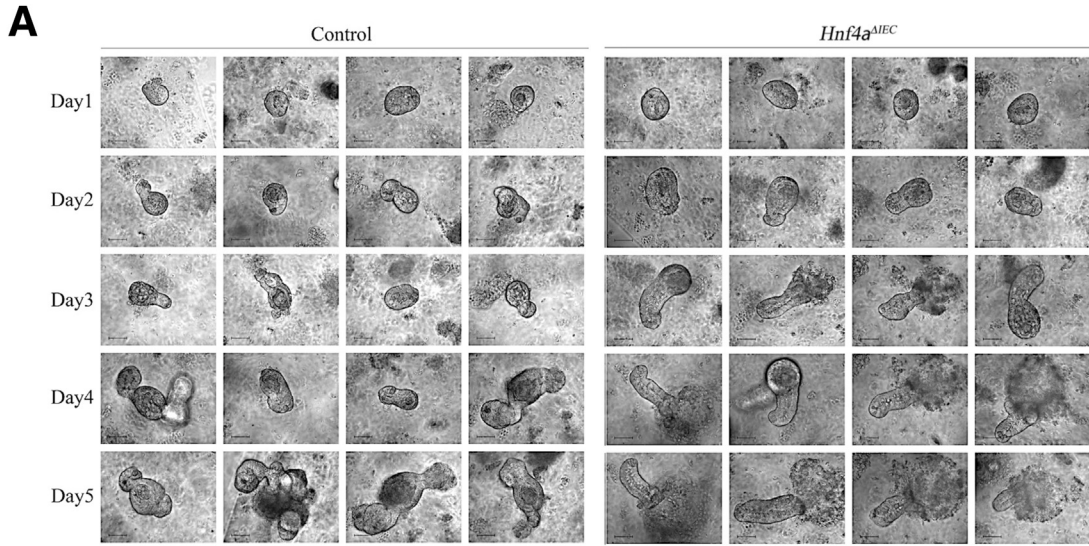


Figure 1. Decreased Wnt3 expression in jejunal crypts depleted for HNF4 α . (A) Crypts were isolated from jejunum of control and *Hnf4a*^{ΔIEC} mice, and total RNA was isolated. RT-qPCR analysis was performed to quantify ISC (*Lgr5*, *Ascl2*, and *Olfm4*), proliferative cell (*Ccnd1* and *Myc*), and Paneth cell (*Lyz*, *Wnt3*, and Defensin) markers (n = 5 for controls, n = 6 for *Hnf4a*^{ΔIEC}). (B) WNT3, HNF4 α , and actin protein levels in jejunal crypts isolated from control and *Hnf4a*^{ΔIEC} mice were assessed by Western blot (n = 2 for control, n = 4 for *Hnf4a*^{ΔIEC}). ns, not significant; *P ≤ .05; **P ≤ .01.

next assessed whether the transcriptomic changes observed in 4OHT-treated *Hnf4a*^{ΔIEC-ind} jejunal enteroids affected the fate of IECs. We performed gene set enrichment analysis (GSEA) to compare overall changes in the transcriptome of these *Hnf4a*-deleted jejunal enteroids with each specific consensus transcriptomic signature of IEC lineages previously captured by single-cell RNA-seq.³³ GSEA analyses of transcriptomic changes in jejunal enteroids that occurred 2 days after *Hnf4a* deletion indicated a robust reduction in gene signatures for Paneth cells, ISCs, and differentiated enterocytes (Figure 4A). In contrast, tuft and goblet gene signatures were significantly enriched 2 days after *Hnf4a* deletion in the jejunal enteroids (Figure 4B), whereas enterocyte progenitor gene signature was not significantly altered (Figure 4C). Similar observations were obtained 4 days after *Hnf4a* deletion (Figure 5A and B), apart from a significant reduction in enterocyte progenitor gene signature and an increase in enterocyte gene signature (Figure 5C). The apparent changeover in enterocyte gene signatures between day 2 and day 4 after *Hnf4a* deletion is intriguing and could be explained by compensatory mechanisms that may operate over time. To this end, HNF4 γ represents a strong candidate because it was previously reported to compensate the loss of HNF4 α on enterocyte gene regulation.^{23–25} Because we observed a reduction in Wnt3

expression and Paneth cell gene signature with a phenotype reminiscent of that of enteroids lacking *Wnt3*, Paneth cells,^{2,7} we further explored the biological impact of these changes with a focus on Paneth cells. Immunofluorescent detection of lysozymes confirmed the occurrence of few Paneth cells in *Hnf4a*-deleted jejunal enteroids compared with that in controls (Figure 6A). We next used combined pharmacologic treatment of jejunal enteroids to commit them to differentiate into Paneth cells, as has been described previously.³⁴ *Hnf4a*^{ΔIEC-ind} jejunal enteroids were treated with an inhibitor of glycogen synthase kinase 3 β (CHIR), combined with an inhibitor of Notch (DAPT), whereas control *Hnf4a*^{ΔIEC-ind} jejunal enteroids were maintained with epidermal growth factor, noggin, and R-spondin 1 culture conditions (designed ENR). As expected, combined CHIR and DAPT treatment led to robust induction of several Paneth cell differentiation markers, including *Wnt3*, *Lyz*, and defensin gene transcripts (Figure 6B, compare blue bars between ENR and CHIR-DAPT conditions for each gene). When *Hnf4a* was deleted from 4OHT supplementation in CHIR- and DAPT-treated *Hnf4a*^{ΔIEC-ind} jejunal enteroids, a significant reduction in most of all Paneth cell marker levels was noted in the enriched population of Paneth cells (Figure 6B, compare blue bars with red bars in CHIR-DAPT conditions). To further evaluate the niche impact of deleting *Hnf4a* in Paneth cells, we



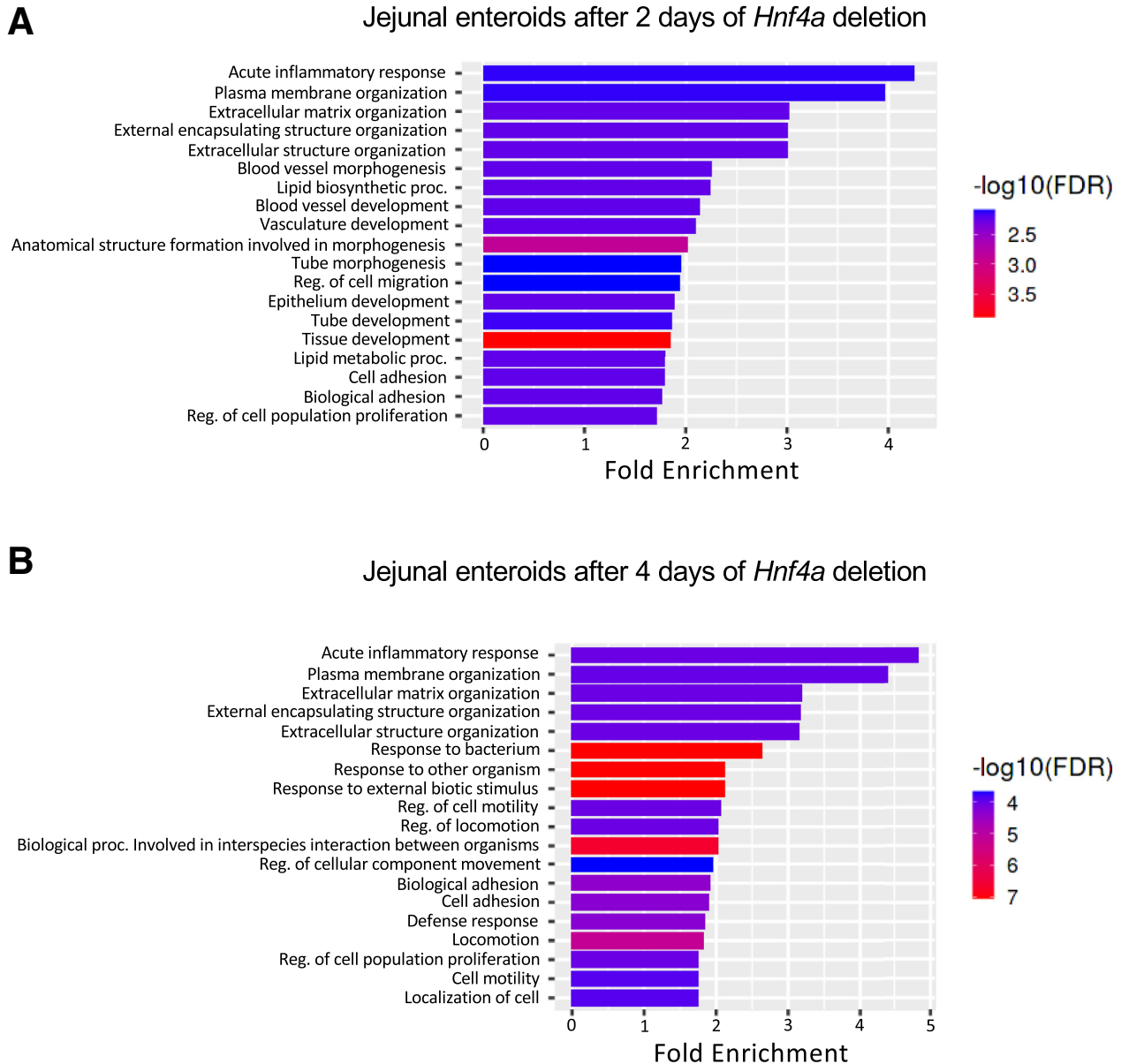


Figure 3. *Hnf4a* deletion in cultured jejunal enteroids leads to transcriptomic changes associated with several biological functions. Total RNA from DMSO- and 4OHT-treated jejunal (*Hnf4a*-deleted) enteroids 2 days (A) and 4 days (B) after deletion was analyzed using RNA-seq. Gene ontology analyses were performed using ShinyGO V0.76 from the list of gene transcripts modulated >2-fold (FDR < 0.05). Significant FDR values are represented as a range of colors, where blue is associated with lower values and red with higher values.

Figure 2. (See previous page). HNF4 α depletion in jejunal enteroids leads to loss of integrity and reduced proliferation rate. (A) Jejunal crypts from control and *Hnf4a* ^{Δ IEC} mice were isolated and embedded in Matrigel to form enteroids. Representative images of at least 3 independent technical replicates of jejunal enteroids at different days after seeding. Scale bar = 50 μ m. (B) *VilCreERT2/Hnf4a*^{lox/lox} jejunal enteroids were treated with DMSO (control) or 4OHT (*Hnf4a* KO) to induce *Hnf4a* deletion. Representative images of at least 3 independent technical replicates of jejunal enteroids at days 2, 4, and 5 revealed similar level of disorganization as that observed in *Hnf4a* ^{Δ IEC} jejunal enteroids. Scale bar = 50 μ m. Total RNA was isolated from DMSO- or 4OHT-induced *VilCreERT2/Hnf4a*^{lox/lox} jejunal enteroids, and RT-qPCR analysis was performed to quantify the expression of *Hnf4a* (C) and *Wnt3* (D) mRNA transcripts. (n = 4 technical replicates performed in independent experiments). (E) EdU incorporation assays using immunofluorescence imaging (E) and flow cytometry (F) of DMSO- or 4OHT-induced *VilCreERT2/Hnf4a*^{lox/lox} jejunal enteroids. (n = 4 technical replicates for the flow cytometry experiment collected in independent experiments). ns, not significant; *P \leq .05; **P \leq .01.

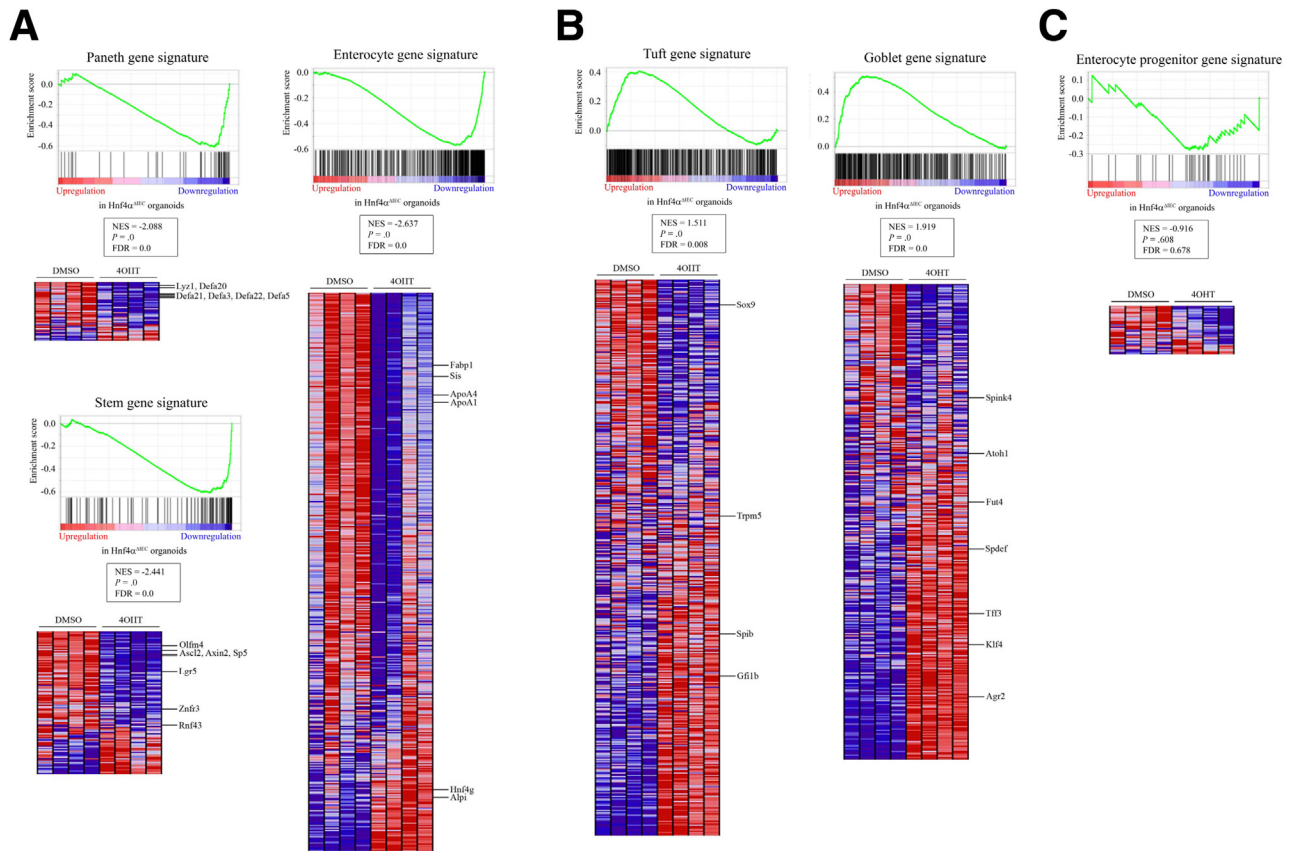


Figure 4. *Hnf4a* deletion in inducible jejunal enteroids causes IECs to rapidly change in gene signatures after 2 days. Total RNA from DMSO- and 4OHT-treated jejunal enteroids 2 days after deletion was analyzed using RNA-seq. GSEA was performed to compare modulated genes with cell-type specific gene signatures of Paneth, ISC, and enterocytes (A), tuft and goblet cells (B) as well as enterocyte progenitors (C). Heat maps, representing genes in the leading-edge subsets, showing expression values, represented as a range of colors. The depicted colors red, pink, light blue, and dark blue were associated with high, moderate, low, and lowest expression levels, respectively. (n = 4 technical replicates performed in independent experiments).

isolated Paneth cells from the jejunum of *Hnf4a*^{ΔIEC} and control mice and combined them with isolated *Lgr5*-eGFP ISCs to grow enteroids. Deletion of *Hnf4a* in Paneth cells did not significantly impact size of resulting enteroids (Figure 7B). However, a strong reduction in crypt-budding structures was observed in enteroids reconstituted with *Hnf4a*-deleted Paneth cells as compared with controls (Figure 7A and C). This observation correlates with the previously described feature of Paneth cell plasma membrane function of Wnt3 during the establishment of defined crypt and villus domains in enteroids.^{7,35} Collectively, these observations indicate a critical role for HNF4 α in the commitment and maintenance of Paneth cell fate as well as their impact on jejunal enteroids crypt-budding in culture.

Wnt Signaling and Subepithelial Mesenchymal Cells Restore HNF4 α -Depleted Jejunal Enteroids Growth

Wnt signaling is crucial for maintaining ISC fitness and intestinal enteroid growth in cultures.^{7,36} We observed a coincidental reduction in Paneth cell numbers and Wnt3 expression upon deletion of *Hnf4a* in jejunal enteroids. Thus, we tested whether the activation of Wnt signaling

could improve enteroid survival after the loss of HNF4 α . The growth of *Hnf4a*-deleted jejunal enteroids was rescued by Wnt3a supplementation, with a resulting cystic phenotype seen in both mutant and control enteroid cultures (Figure 8A). This observation is reminiscent of the intestinal enteroids activated by Wnt signaling.⁷ The size of *Hnf4a*-deleted jejunal enteroids was increased by 1.9-fold ($P < .0001$) under these conditions (Figure 8B). To better characterize the impact of Wnt signaling activation at the molecular level, transcriptomic analyses were performed in *Hnf4a*^{ΔIEC-ind} jejunal enteroids with or without gene deletion in the presence of Wnt3a supplementation over a total period of 2 days. These analyses showed that the loss of HNF4 α significantly altered the expression of 527 gene transcripts when stimulated with Wnt3a (Supplementary Table 3). GSEA analyses indicated that the overall Paneth cell transcriptome was no longer significantly altered in the deleted *Hnf4a*^{ΔIEC-ind} jejunal enteroids when treated with Wnt3a (Figure 8C). This observation is in accordance with the previous literature regarding the dependence of Paneth cells on Wnt signaling for differentiation.^{7,14} Interestingly, the activation of Wnt signaling did not affect the goblet and tuft cell gene signatures caused by the loss of HNF4 α

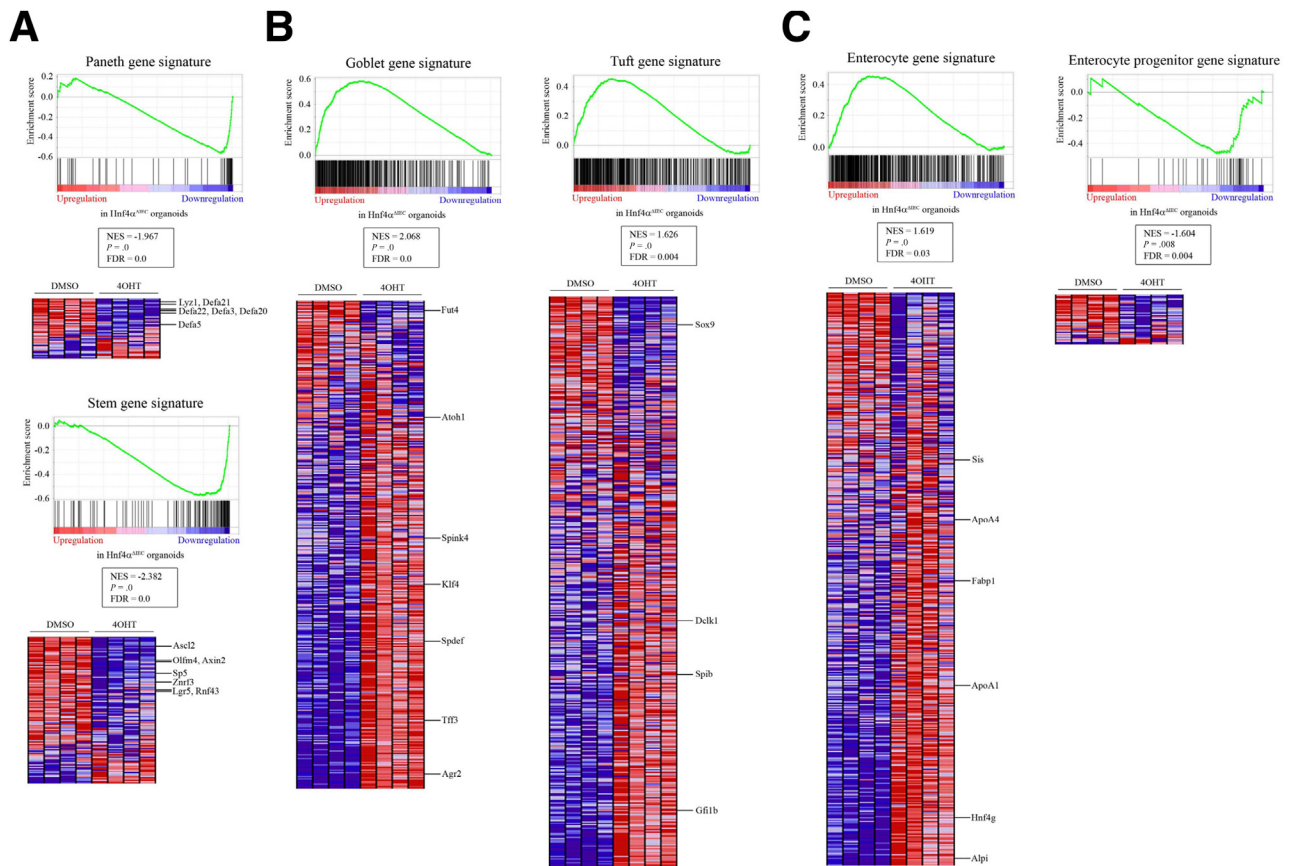


Figure 5. *Hnf4a* deletion in inducible jejunal enteroids maintains IECs change of gene signatures after 4 days. Total RNA from DMSO- and 4OHT-treated jejunal enteroids after 4 days of deletion was analyzed using RNA-seq. GSEA was performed to compare modulated genes with cell-type specific gene signatures of Paneth and ISC (A), goblet and tuft cells (B), as well as enterocyte progenitors and differentiated cells (C). Heat maps, representing genes in the leading-edge subsets, showing expression values, represented as a range of colors. The depicted colors red, pink, light blue, and dark blue were associated with high, moderate, low, and lowest expression levels, respectively. (n = 4 technical replicates performed in independent experiments).

(Figure 8D). Although supplementation with Wnt3A corrected a few ISC-associated gene transcripts found to be modulated in the absence of HNF4 α , GSEA analysis indicated that this cell gene signature was still significantly reduced under these conditions (Figure 8E). A significant reduction in enterocytes gene signature was also observed, whereas enterocyte progenitor gene signature was not altered under these conditions (Figure 8F).

The mesenchymal niche is required for ISC preservation by subepithelial telocytes⁶ and recently characterized trophocytes,⁵ with both relaying Wnt signals to crypt intestinal epithelial cells. To evaluate whether the viability of jejunal enteroids lacking *Hnf4a* could be rescued by such cellular interactions, we cultured enteroids with primary mesenchymal cells derived from human fetal ileum and previously shown to support IEC differentiation.³⁷ Dissociated jejunal crypts from both control and *Hnf4a* ^{Δ IEC} mice were cultured with or without mesenchymal cells engineered to express green fluorescent protein (GFP). Although *Hnf4a* ^{Δ IEC} jejunal enteroids started to degenerate by day 4, co-culture with mesenchymal cells promoted their survival and led to the formation of large spheroidal, proliferating

epithelial structures with phenotypic similarities to control jejunal enteroids co-cultured under the same conditions (Figure 9A). Interestingly, large GFP⁺ cells with phenotypic characteristics of telocytes, including extended cell bodies and telopodes,³⁸ were found in close proximity to the growing epithelial spheroids (Figure 9A). High-resolution microscopy confirmed multiple contact points between the telopodes and epithelial cells contained in these spheroids (Figure 9B). Similar to Wnt3a-supplemented conditions, the size of *Hnf4a*-deleted jejunal enteroids was increased by 1.7-fold in presence of mesenchymal cells ($P < .01$) (Figure 9C). To better characterize the impact of co-cultures on the mouse *Hnf4a* ^{Δ IEC} jejunal enteroids transcriptome as well as to gain insight into the specific nature of human primary mesenchymal cells behavior when placed in the presence of enteroids, we performed mixed-species RNA-seq that allowed for the investigation of the evolutionary divergence of mRNA within cell populations without having to undergo the process of cell sorting.³⁹ A mouse-specific transcriptomic analysis identified 700 gene transcripts that were significantly modulated in *Hnf4a* ^{Δ IEC} jejunal enteroids co-cultured with mesenchymal cells, when compared with

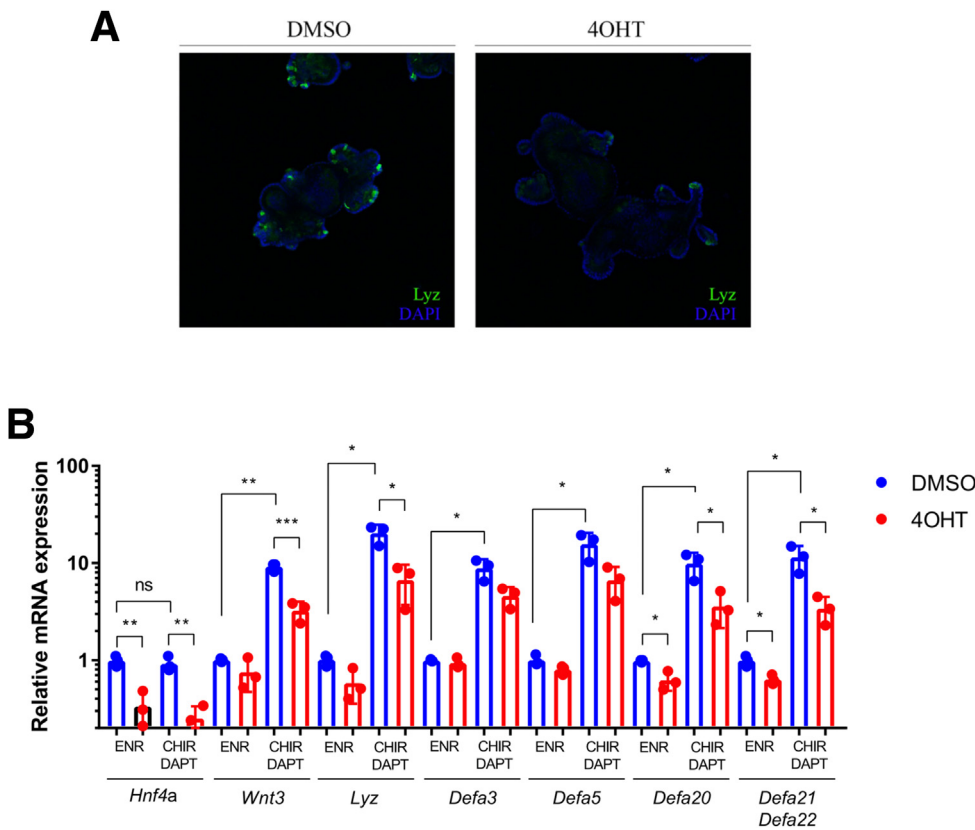


Figure 6. Paneth cells are reduced after deletion of *Hnf4a* in jejunal enteroids. (A) Green fluorescence of lysozyme-positive cells in DMSO- and 4OHT-treated jejunal enteroids exposed for 4 days. Nuclei are stained blue with DAPI. (B) RNA from normal (ENR) and Paneth-like (CHIR-DAPT) enteroids, deleted or not for *Hnf4a*, was extracted, and RT-qPCR experiments were conducted to assess Paneth cell marker expression. A significant reduction in Paneth cell markers was observed in the absence of HNF4 α in Paneth-like enteroids. (n = 3 technical replicates performed in independent experiments). ns, not significant; * $P \leq .05$; ** $P \leq .01$; *** $P \leq .001$.

control jejunal enteroids co-cultured under the same conditions (Supplementary Table 4). Although these mesenchymal cells restored the growth and survival of *Hnf4a* ^{Δ IEC} jejunal enteroids, GSEA analyses indicated that the Paneth cell transcriptome was still significantly altered in deleted *Hnf4a* ^{Δ IEC-ind} jejunal enteroids in co-cultures (Figure 9C). As observed in the Wnt3 rescue experiments, the presence of mesenchymal cells did not restore the goblet and tuft cell gene signature changes caused by the loss of HNF4 α (Figure 9D). The same observation was also made for the ISC population (Figure 9E). A significant reduction in enterocyte gene signature was also observed, whereas enterocyte progenitor gene signature was induced under these conditions (Figure 9F).

We next characterized the specific changes occurring in human mesenchymal cells when co-cultured with mouse jejunal enteroids. Mixed-species RNA-seq analysis revealed that 1,290 human gene transcripts were significantly modulated in mesenchymal cells put in contact with the mouse jejunal enteroids (Supplementary Table 5). A closer look at the Wnt and BMP pathway signals, previously annotated as specific markers to discriminate the specific nature of the mesenchyme-resident population of cells,^{6,40} indicated an enrichment for a telocyte signature among these cells (Supplementary Table 5). *PDGFRA*, *FOXL1*, *WNT4*, *WNT5A*, *BMP2*, *BMP4*, *BMP5*, and *BMP7* gene transcripts were robustly induced, whereas *GREM1*, *RSPO2*, and *RSPO3* were silenced in these co-culture conditions (Figure 10). Overall, these observations confirmed the efficacy of

mesenchymal culture containing telocyte-like cells in ensuring a sustainable environment for epithelial maintenance in the absence of HNF4 α and Wnt3 depletion, a situation reminiscent of *Hnf4a* ^{Δ IEC} in vivo jejunal conditions. In addition, these observations suggest that a functional crosstalk exists between epithelial and subepithelial mesenchymal cells regarding enrichment of these telocyte-like cells.

Wnt3 and Mesenchymal Culture Containing Telocyte-like Cells Restore Transcriptomic Changes in the Absence of HNF4 α

Because *Hnf4a* deletion in the murine small intestine in vivo poorly influences the transcriptome, we assessed the number of genes critically dependent on HNF4 α expression in jejunal enteroids supplemented or not with Wnt3a or human mesenchymal culture containing telocyte-like cells. Of the 2,137 gene transcripts that were up-regulated in jejunal enteroids 2 days after *Hnf4a* deletion, 311 of them were still significantly modulated after Wnt3a supplementation (Figure 11A, left gray and green circles). Similarly, only 155 gene transcripts were still significantly modulated after Wnt3a supplementation when compared with the 2,026 down-regulated gene transcripts before Wnt3a supplementation (Figure 11B, left gray and green circles). Thus, Wnt3a rescued ~89% of transcriptomic changes in the absence of HNF4 α . A similar analysis was performed on jejunal enteroids 4 days after *Hnf4a* deletion in the presence

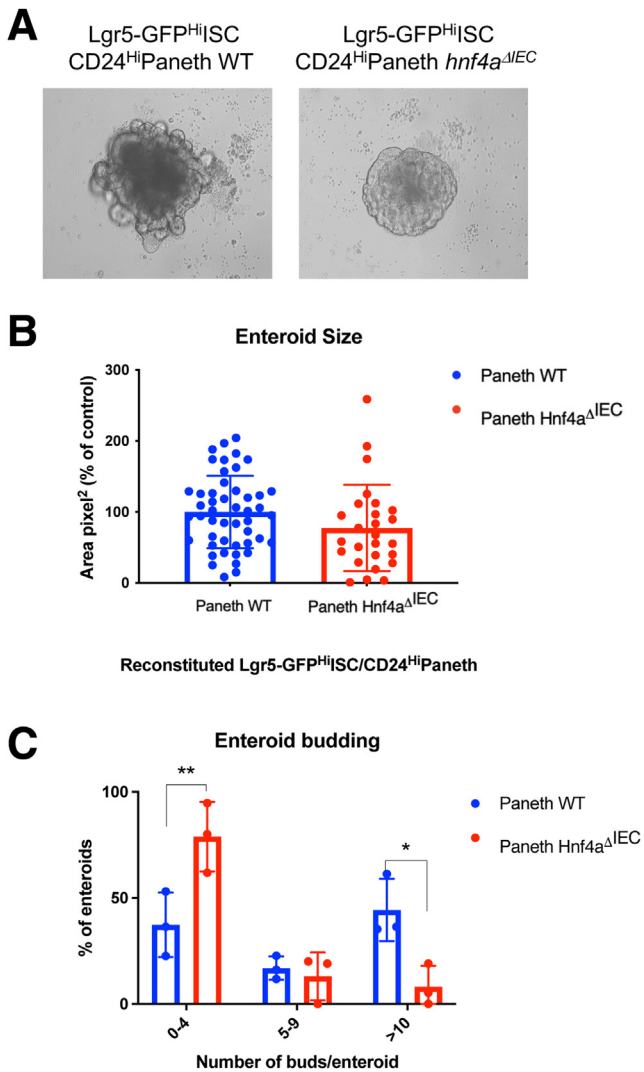


Figure 7. Reassociation of *Hnf4a*-deleted Paneth cells with ISCs impairs crypt budding of enteroids. ISCs (GFP^{Hi}) were sorted and re-associated with wild-type (WT) or *Hnf4a*-deleted Paneth cells (CD24^{Hi}) to form enteroids. (A) Representative image of 3 technical replicates performed in independent experiments of reconstituted jejunal enteroids after 12 days of reassociation. (B) Graph showing enteroids size. Areas (pixel²) were assessed using ImageJ. (N = 2; n = 48 for enteroids containing WT Paneth cells, and n = 26 for enteroids containing *Hnf4a*-deleted Paneth cells). (t test; ns, not significant). (C) Bar graph representing the number of buds per reconstituted enteroid. Enteroids were divided into 3 groups according to their number of buds: 0–4, 5–9, or more than 10 buds. (N = 3, n = 65 for enteroids containing WT Paneth cells, and n = 41 for enteroids containing *Hnf4a*-deleted Paneth cells). (Two-way analysis of variance; *P ≤ .05; **P ≤ .01).

or absence of mesenchymal culture containing telocyte-like cells. Of the 2,678 gene transcripts that were up-regulated in the absence of HNF4 α , 257 were still significantly modulated in the presence of mesenchymal culture containing telocyte-like cells (Figure 11A, right purple and blue circles). Similarly, only 153 gene transcripts were still significantly modulated in the presence of mesenchymal

culture containing telocyte-like cells, when compared with 1,836 down-regulated gene transcripts in the absence of mesenchymal culture containing telocyte-like cells (Figure 11B, right purple and blue circles). Mesenchymal culture containing telocyte-like cells was able to rescue ~91% of the transcriptomic changes in the absence of HNF4 α . A comparison of gene transcripts modulated in the absence of HNF4 α and not rescued during both Wnt3a and mesenchymal culture containing telocyte-like cells exposure identified a total of 116 up-regulated gene transcripts (Figure 11A) and 37 down-regulated gene transcripts (Figure 11B) (Supplementary Table 6). These observations support that the epithelial or mesenchymal niche is required for jejunal enteroids to restore their transcriptomic changes associated with the loss of HNF4 α . In addition, only a few genes have emerged as intrinsic HNF4 α -dependent targets under these conditions, a situation reminiscent of the in vivo non-pathologic process where telocytes can physiologically overcome defects emerging from the intestinal epithelial niche.

HNF4 α Acts as Upstream Transcriptional Regulator of Wnt3

The observation that Wnt and mesenchymal culture containing telocyte-like cells were able to restore most of the transcriptomic changes caused by HNF4 α depletion suggests the existence of intimate crosstalk between HNF4 α and transcriptional regulators affected by Wnt signaling. Consistent with this, HNF4 α has been reported to physically interact with TCF4⁴¹ and to co-localize with certain common genomic DNA sequences.⁴² Of the remaining gene transcripts that were not rescued after Wnt3a or mesenchymal culture containing telocyte-like cells exposure, we found that *Wnt3* transcripts were still reduced by >40% (FDR < 0.05) in deleted *Hnf4a*^{ΔIEC-ind} jejunal enteroids when compared with that in control jejunal enteroids under Wnt3a treatment or by >98% (FDR < 0.05) in the presence of mesenchymal culture containing telocyte-like cells (Supplementary Table 6). Interestingly, HNF4 α directly bound to an upstream region in *Wnt3* gene promoter, in association with active H3K27Ac chromatin mark for this gene at this position, as well as in a region of intron 4, as visualized by chromatin immunoprecipitation sequencing (ChIP-seq) analysis previously performed in isolated mouse jejunal epithelial cells (Figure 12A).^{43,44} To further test whether HNF4 α can regulate *WNT3* directly, we took advantage of an IEC line engineered to conditionally express the HNF4 α 2 isoform.⁴⁵ *WNT3* transcript expression was found up-regulated when this isoform was induced in HCT116 cells (Figure 12B). HNF4 α 2 directly bound the *WNT3* gene as visualized by ChIP-seq analysis previously performed in HCT116 cells and was conditionally induced to express this isoform⁴² (Figure 12C). HNF4 α 2 peaks observed in introns 1 and 4 of the *WNT3* gene correlated with active H3K27Ac chromatin marks for this gene at these positions (Figure 12C). Sequence analysis overlapping these enriched regions predicted the presence of 5 binding sites spanning 4,880 base pairs in introns 1 and 5 additional sites spanning 4,259 base pairs in intron 4 (Figure 12D).

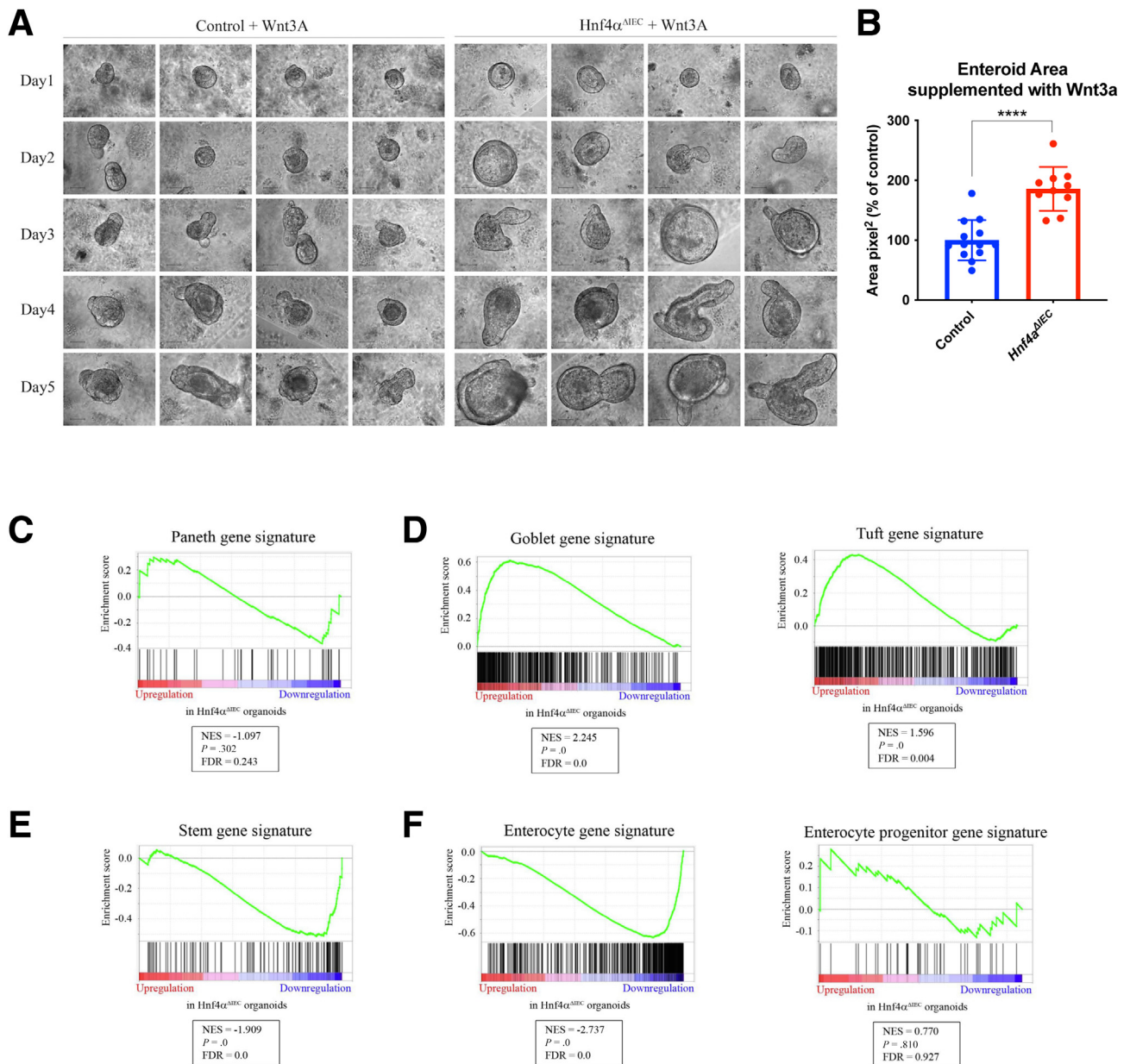


Figure 8. Wnt3a supplementation rescues *Hnf4α^{ΔIEC}* jejunal enteroid survival without correcting changes in goblet and tuft cell gene signatures. (A) Jejunal enteroids from control and *Hnf4α^{ΔIEC}* mice were cultured for 5 days in the presence of Wnt3a in the culture medium. Representative images of enteroids from at least 3 independent technical replicates at different time points indicated that addition of Wnt3a rescued the survival of *Hnf4α^{ΔIEC}* jejunal enteroids. Scale bar = 50 μ m. (B) Areas (pixel²) of jejunal enteroid size were assessed using ImageJ and expressed as percentage of control enteroids (* $P \leq .01$). RNA-seq data obtained were analyzed using GSEA software for comparison with Paneth cell gene signature (C), goblet cell and tuft cell gene signatures (D), ISC gene signature (E), as well as differentiated and progenitor enterocyte gene signatures (F).

Collectively, these observations support that HNF4 α acts as an upstream transcriptional regulator of the *Wnt3* gene, together with an impact on autocrine epithelial Wnt3 signaling and Paneth cell fate.

Discussion

The intestinal epithelium is a self-renewing system that depends on ISCs to replenish daughter-differentiated cells.

Stem cell functions are supported by an adjacent niche established from the input of multiple and distinct sub-epithelial and epithelial cell types specialized in the production of regulatory signals, with considerable overlap and redundancy among them.⁴⁰ In addition, plasticity within progenitors and mature cells can cause them to dedifferentiate and replace damaged ISCs during epithelial regeneration after injury.^{46,47} All of these redundant mechanisms have evolved to maintain intestinal epithelial homeostasis,

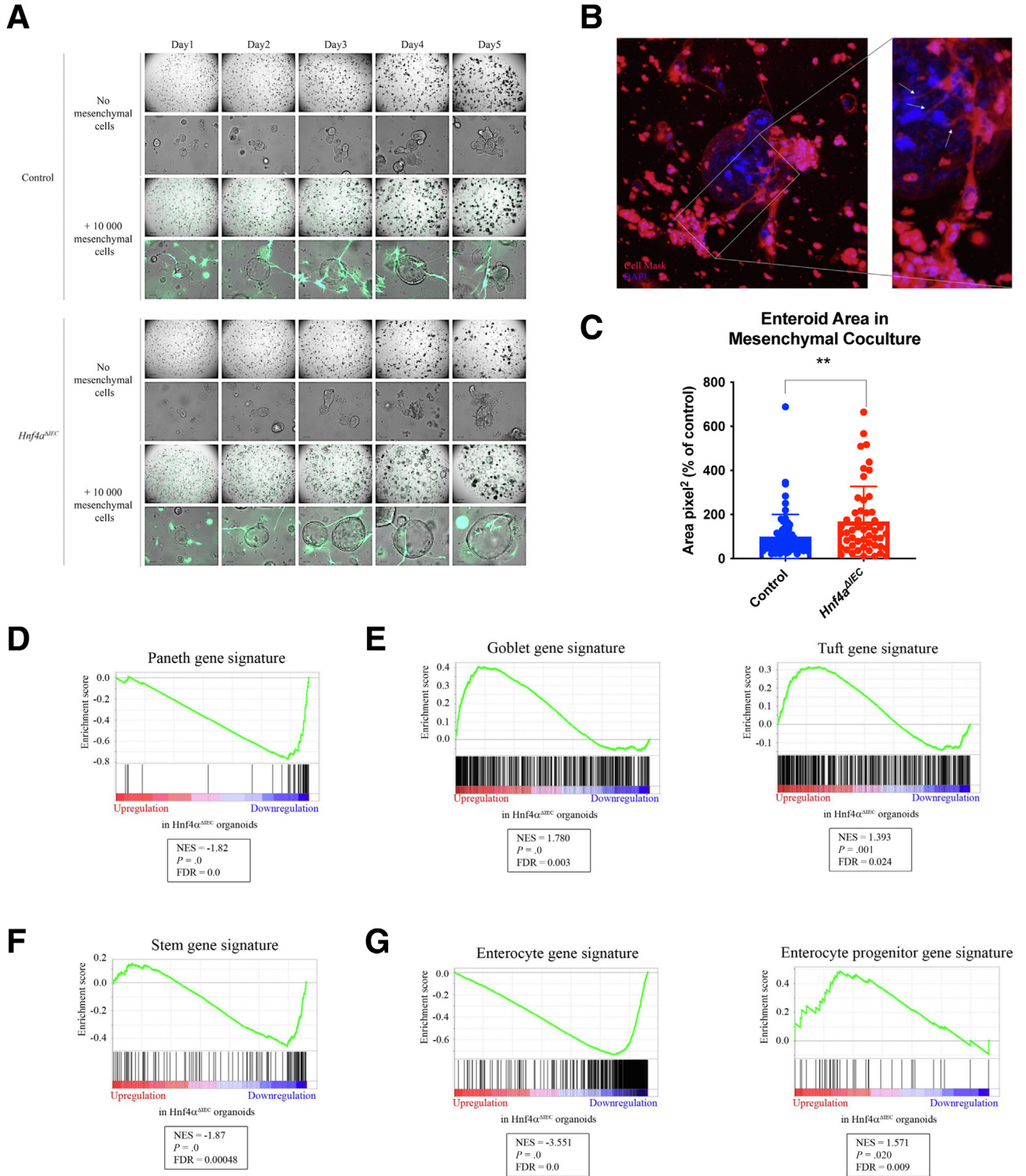


Figure 9. Human primary mesenchymal cells rescue *Hnf4a^{ΔIEC}* jejunal growth in culture. (A) Crypts from control and *Hnf4a^{ΔIEC}* mice were maintained in culture, with or without human mesenchymal cells. They were kept under culture for 5 days, and images were acquired each day using a Zeiss Celldiscorer 7. Representative images of 2 independent technical replicates at 2 different original magnifications (2.5× and 20×) are shown. Scale bar = 500 μm for 2.5× magnification and 50 μm for 20× magnification. (B) Live co-culture sample stained at day 5 using CellMask Deep Red Plasma Membrane Stain (red) and Hoechst 33342 (blue). Three-dimensional imaging was performed using confocal microscopy. One enteroid surrounded by mesenchymal cells is shown. White dashed box emphasizes a mesenchymal cell that displays elongated telopods in close contact with epithelial cells (white arrows). (C) Areas (pixel²) of jejunal enteroid size were assessed using ImageJ and expressed as percentage of control enteroids (*****P* ≤ .0001). Mixed-species RNA-seq data obtained were analyzed using GSEA software for comparison with Paneth cell gene signature (D), goblet cell and tuft cell gene signatures (E), ISC gene signature (F), as well as differentiated and progenitor enterocyte gene signatures (G).

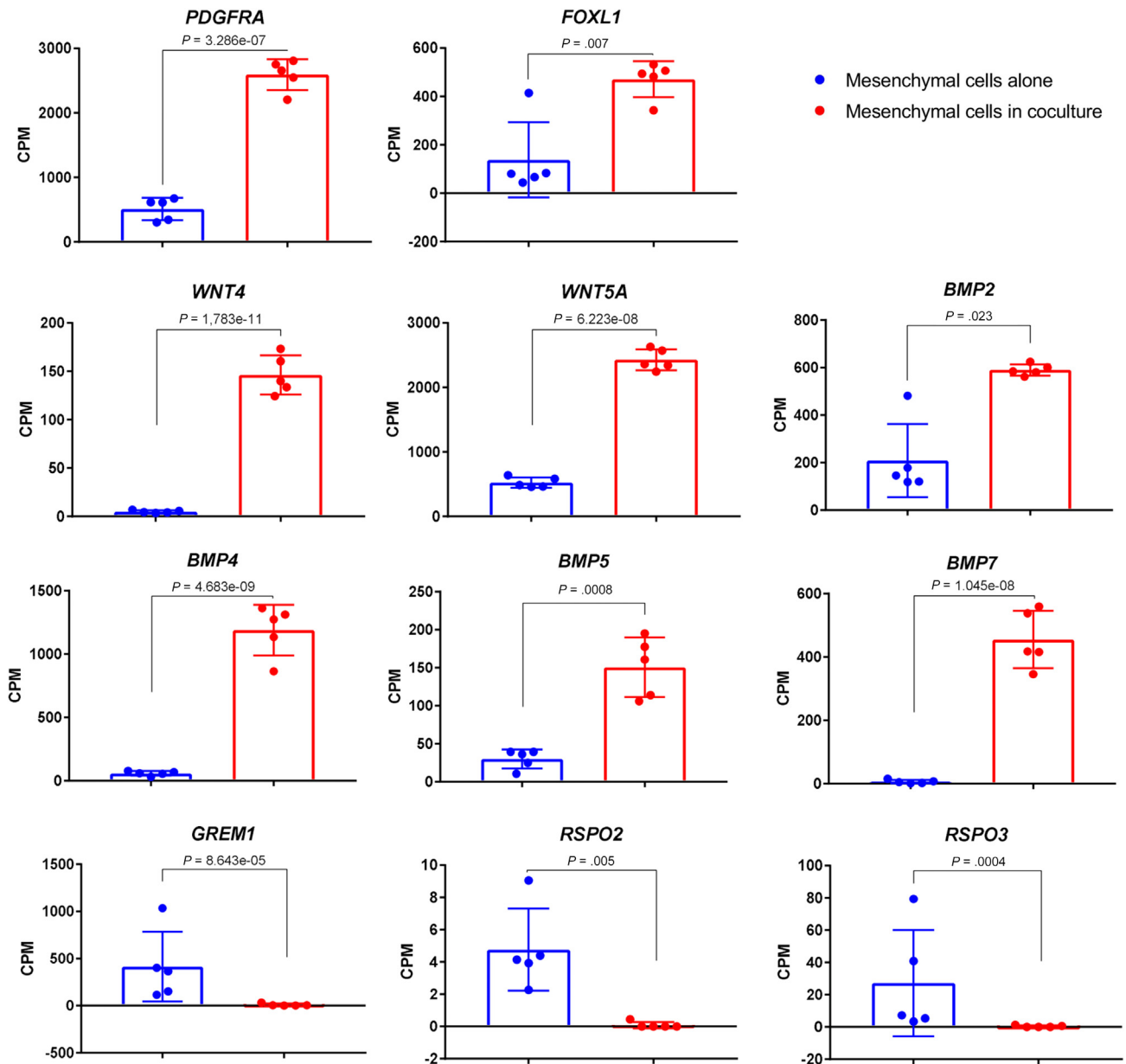


Figure 10. Human primary subepithelial mesenchymal cells become enriched in telocyte-like cells in presence of mouse jejunal enteroids. Gene transcript expression of various mesenchymal cell markers was compared using mixed-species RNA-seq in human mesenchymal cells cultured with or without mouse jejunal enteroids (n = 5 technical replicates performed in independent experiments).

regardless of the nature of threatening environmental cues. Herein, we adopted multiple *ex vivo* strategies to investigate the role of epithelial HNF4 α in maintenance of the intestinal niche. On the basis of the similarities observed among our different experimental systems, we observed that survival of jejunal enteroids deleted for *Hnf4a* can be rescued in culture with either exogenous Wnt3a or mesenchymal cells in a co-culture environment. These rescue experiments also corrected ~90% of the jejunal enteroid transcriptome specifically modified after *Hnf4a* deletion. Paneth cell gene signature was reduced in jejunal enteroids deleted for *Hnf4a*, and this signature remained reduced when co-cultured with mesenchymal cells. However, the supplementation of jejunal

enteroids deleted for *Hnf4a* with Wnt3a restored Paneth cell gene signature, probably because Paneth cells are dependent on Wnt signaling for differentiation.^{7,14} Finally, goblet and tuft cells gene signatures remained elevated in all tested biological setups. It thus appears that HNF4 α opposes these signatures, but whether this impacts on intestinal biology remains to be further investigated.

Our findings highlight a previously unappreciated and novel role for HNF4 α alone in regulating Paneth cells via Wnt3 and support that HNF4 paralogs are not entirely redundant for intrinsic IEC functions when secluded from multiple environmentally driven compensatory mechanisms in the intestine.^{23,24} This strong phenotype manifested only

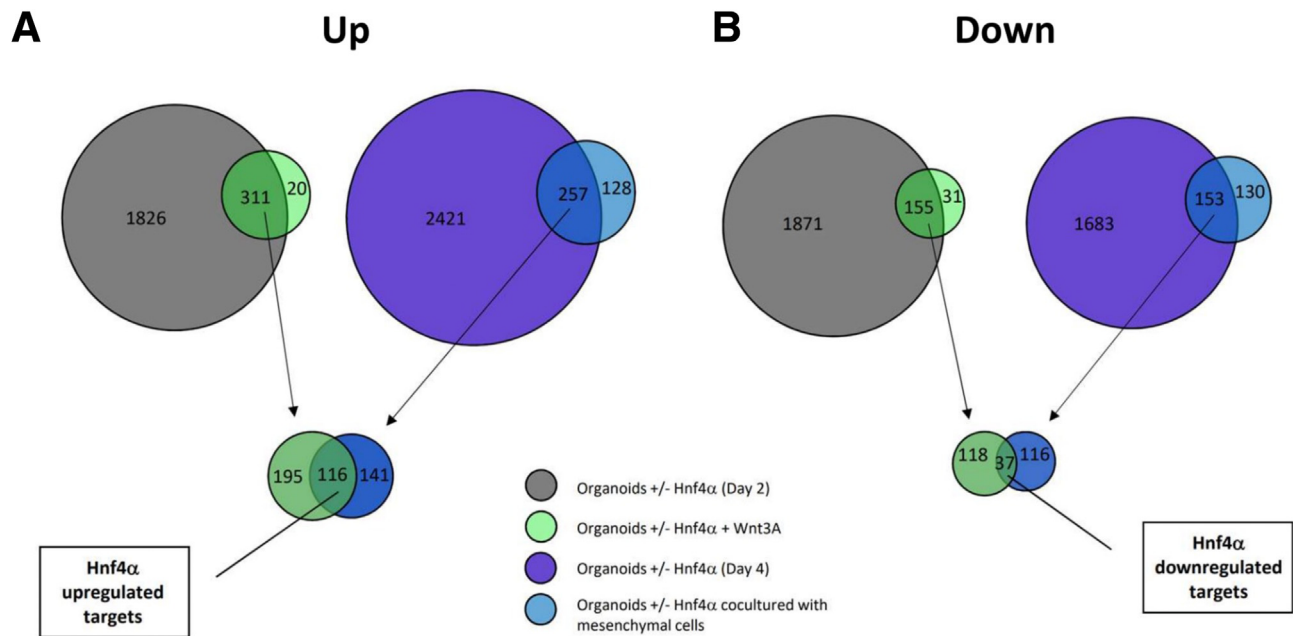


Figure 11. Mesenchymal culture containing telocyte-like cells and Wnt signaling rescue most of transcriptomic changes observed in *Hnf4a*-deleted jejunal enteroids. (A) Total RNA from DMSO- and 4OHT-treated jejunal (*Hnf4a*-deleted) enteroids 2 (with or without Wnt3a) or 4 days (with or without mesenchymal cells) after deletion was analyzed by RNA-seq. Venn diagrams were used to display comparisons of gene transcript levels that were significantly up-regulated (A) or down-regulated (B) in these conditions (FDR < 0.05). Gene transcripts that were still significantly modulated in *Hnf4a*-deleted jejunal enteroids put in the presence of Wnt3a (green circles) or mesenchymal cells (blue circles) were compared using Venn diagrams. This analysis identified 116 up-regulated genes and 37 down-regulated genes affected by the loss of HNF4a and that were not rescued by either Wnt3a or mesenchymal cells.

a few days after *Hnf4a* deletion in the growing jejunal enteroids, an observation that is controversial considering previous literature. Chen et al²³ observed longer budding crypts in HNF4 α -depleted enteroids, without noting changes in cell growth. Similar to our findings, Montenegro-Miranda et al³⁰ reported that HNF4 α is required to allow enteroid propagation in culture. However, they concluded that supplementation of HNF4 α -depleted enteroids with Wnt3a only partially maintained their survival and failed to ensure their maintenance after passage. Activation of Wnt signaling with either Wnt3 α or CHIR allowed us to maintain HNF4 α -deficient enteroid growth for several passages, indicating that restoration of the Wnt epithelial niche was sufficient to restore ISC function under these conditions.

HNF4 α depletion does not severely affect either the small intestine transcriptome or homeostasis under strict normal physiological conditions, mainly because of the redundant roles of HNF4 α and HNF4 γ .^{18,23,24} However, HNF4 α depletion in enteroids devoid of a mesenchymal niche led to rapid changes in gene ontology functions associated with inflammation, cell migration, and lipid metabolic processes. These functions were altered in *Hnf4a* ^{Δ IEC} mice exposed to radiation,³⁰ inflammatory stress,^{29,48} or a high-fat diet.⁴⁹ Collectively, these observations indicate that the study of HNF4 α function in enteroids could be an asset in dissecting the contribution of the epithelial versus mesenchymal niche contribution to intestinal homeostasis, particularly in conditions that mimic pathologic situations.

Although the role of Paneth cells in maintaining ISC function overlaps with that of mesenchymal cells in the intestine, it is still unclear how these cellular entities interact with this end under intestinal injury and pathologic conditions. One important aspect of our findings is the potential of jejunal enteroids to stimulate subepithelial mesenchymal cells to become telocyte-like cells. This observation implies the existence of specific crosstalk between epithelial cells and neighboring mesenchymal cells. Elucidating the specific nature of the molecules involved in this process represents an exciting future direction.

It is now well-established that telocytes constitute the intestinal stem cell niche under normal physiological conditions. However, their function during intestinal pathologies requires careful investigation. Paneth cell dysfunction can initiate intestinal inflammation,⁵⁰ and Wnt factors play a central role in epithelial regeneration during intestinal inflammation⁵¹ and cancer.⁵² Because of the well-documented *HNF4A* alterations in gut diseases,^{27,53} our findings shed light on a novel molecular cascade of physiological importance in gut biology and diseases.

HNF4 paralogs are crucial for the regulation of intestinal epithelial genes during fetal⁵⁴ and adult life.²³ One important conclusion from these reports is that both HNF4 α and HNF4 γ are redundant for gene transcription. Although we observed profound transcriptomic changes after *Hnf4a* deletion in enteroids, our data support that a large

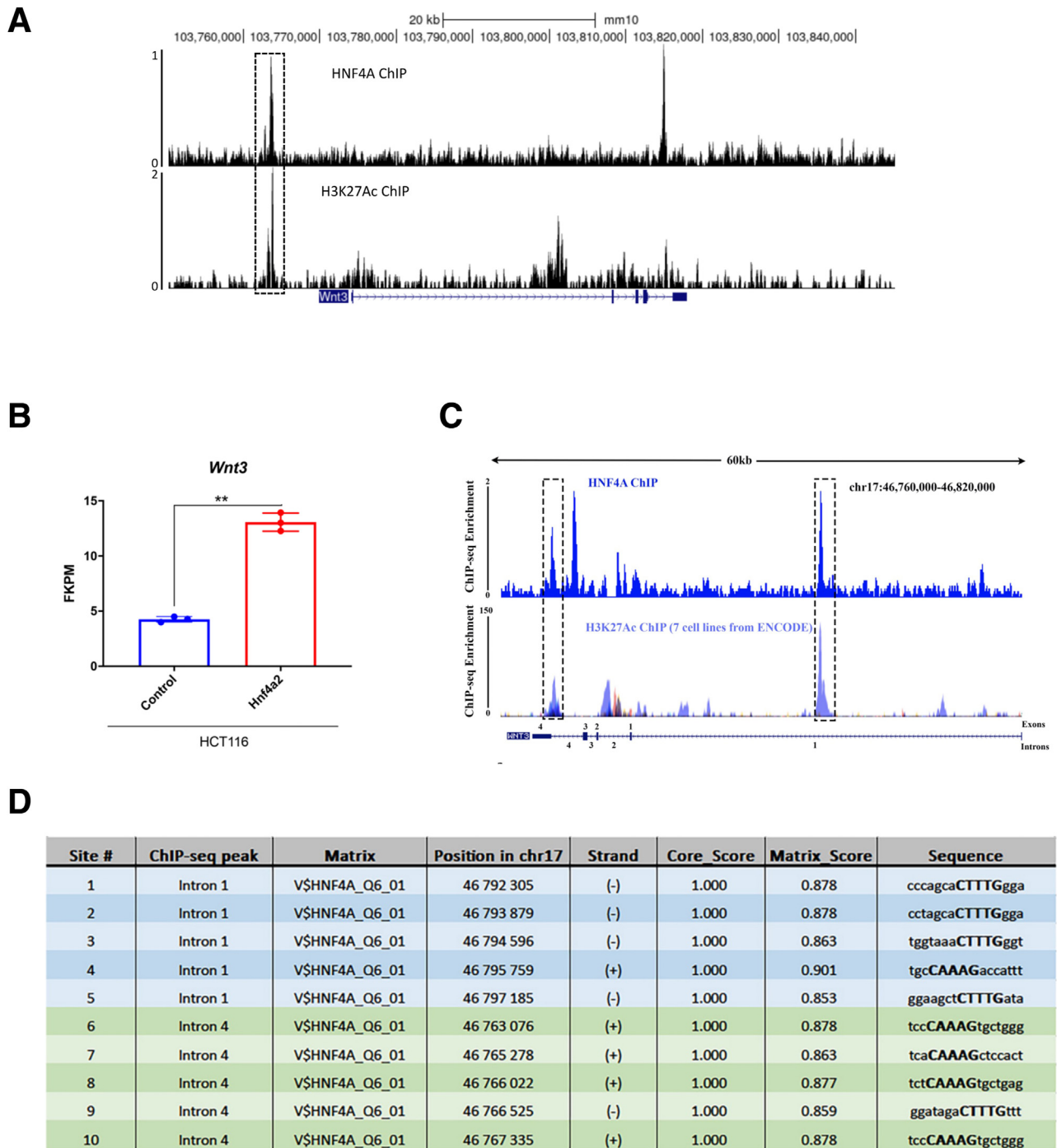


Figure 12. HNF4 α acts as an upstream regulator of Wnt3. (A) ChIP-seq tracks of HNF4 α occupancy on Wnt3 from isolated mouse jejunal epithelial cells. Upstream HNF4 α binding site overlaps with an H3K27Ac mark (dashed rectangle). (B) WNT3 gene transcript expression obtained by RNA-seq in HCT116 cells overexpressing or not HNF4 α 2 (n = 3 technical replicates performed in independent experiments). (C) ChIP-seq tracks of HNF4 α occupancy on WNT3 in HCT116 cells. HNF4 α binding overlaps regions enriched for the H3K27Ac mark in different cell lines (dashed rectangles). (D) Distribution of HNF4 α binding sites from HNF4 α ChIP-seq peaks in introns 1 (chr17:46 792 000-46 798 000) and 4 (chr17:46 763 000-46 768 000) of the Wnt3 gene. (**P \leq .01).

proportion of these genes are not direct targets of HNF4 α . Consistent with this finding, Wnt3a supplementation restored the expression of a multitude of transcripts that were altered in HNF4 α -depleted enteroids. Wnt signaling transduces gene expression via nuclear translocation of the

β -catenin effector, which in turn forms a complex with members of the TCF/LEF family to modulate gene transcription.⁵⁵ HNF4 α functionally interacts with both β -catenin and TCF4 in the liver, an interaction that antagonizes the transcription of their respective gene target

repertoire.⁵⁶ A study conducted in a human colon cancer cell line showed that HNF4 α isoforms can either recruit TCF4 to the chromatin or compete with it for chromatin binding, depending on the structure of the targeted gene promoters and the specificity of HNF4 α P1 or P2 isoforms.⁴² Negative regulatory feedback also exists between β -catenin and HNF4 α P1 isoforms in colon cancer cell lines.⁵⁷ It is thus possible that HNF4 α interacts with β -catenin to influence the expression of some of these transcripts in an indirect manner. Nevertheless, our data strongly support that *Wnt3* is a direct transcriptional target of HNF4 α . Reports identifying specific transcription factors regulating *Wnt3* expression are scarce. A recent study performed in the *Hydra* polyps convincingly highlighted β -catenin and Sp5 to regulation of the *HyWnt3* promoter.⁵⁸ To our knowledge, HNF4 α is the first transcription factor discovered that regulates *Wnt3* in the intestinal epithelium.

The analysis of our transcriptomic data suggests a crucial role for HNF4 α in determining IEC fate in the absence of a compensatory source of mesenchymal Wnts. Our observations are consistent with previous findings that Wnt signaling is required for both differentiation of Paneth cells and maintenance of Lgr5+ stem cells, while blocking goblet cell and mature enterocyte differentiation.³⁴ We did not find evidence of an overall modulation in Notch signaling in jejunal enteroids deleted for *Hnf4a*, conditions that are normally required for goblet cell differentiation but that impede enterocyte maturation.³⁴ On the other hand, Notch activation can force Paneth cells to dedifferentiate into multipotent stem cells to replenish the epithelium.^{11,13} Interestingly, tuft cells have been reported to act as an alternative source of Notch signaling in the crypts of mice in which Paneth cells were depleted.⁵⁹ We cannot exclude the possibility that a specific subclass of progenitors harbored a change in Notch signaling in the absence of HNF4 α , thus affecting goblet and tuft cell fates.

In summary, our data indicated that although HNF4 paralogs are redundant for the transcription of intestinal epithelial genes, HNF4 α alone is crucial to sustain *Wnt3* expression that is specific to Paneth cells of the intestinal epithelium. Disruption of this regulatory loop is important for maintaining the ISC niche in the absence of compensatory mesenchymal signals. Because of the documented importance of Paneth cells, Wnt signaling, and HNF4A integrity in gut diseases, our findings provide new perspectives for further exploration of therapeutic strategies for intestinal epithelial disorders.

Methods

Mice

C57BL/6 12.4Kb*VilCre*⁶⁰ and *VilCreERT2*⁶¹ transgenic mice were bred with *Hnf4a*^{tm1Gonz} (Jackson Laboratories, Bar Harbor, ME; stock number 004665) to obtain 12.4Kb*VilCre/Hnf4a*^{fx/fx} and *VilCreERT2/Hnf4a*^{fx/fx} as previously described.¹⁸ Lgr5-EGFP-ires-CreERT2 mice were purchased from The Jackson Laboratory (stock no. 000664). Breeders and experimental mice were genotyped using polymerase chain reaction. Animals were anesthetized with

ketamine/xylazine (300 mg/kg; 40 mg/kg) before euthanasia. All experiments were performed in accordance with protocols approved by the Animal Research Committee of the Faculty of Medicine and Health Sciences of the Université de Sherbrooke (approval ID number 102-18), in accordance with the Canadian Council on Animal Care.

Crypt Isolation

Crypts were isolated from the jejunum by using EDTA. Briefly, intestines from *VilCre/Hnf4a*^{fx/fx} (*Hnf4a* ^{Δ IEC}) and *Hnf4a*^{fx/fx} (control) were dissected longitudinally, washed thoroughly in phosphate-buffered saline (PBS) once, and cut into 5 mm pieces. Jejunal pieces were then incubated for 20 minutes in 30 mmol/L EDTA on ice. EDTA was replaced with ice-cold PBS, and the tissues were vigorously shaken. Supernatants were then passed through a 70 μ m cell strainer to reserve only the flow-through containing the crypts. The RNA and proteins were extracted after crypt enrichment.

Jejunal Enteroid Culture

Jejunal crypts from *Hnf4a* ^{Δ IEC}, control, and *VilCreERT2/Hnf4a*^{fx/fx} mice were isolated using EDTA and placed in Matrigel (BD Bioscience, Franklin Lake, NJ) to form jejunal enteroids as described previously.⁶² For passaging, jejunal enteroids were removed from the Matrigel and mechanically dissociated using a P200 pipette tip fixed on a 5 mL serologic pipette. To induce deletion of *Hnf4a*, 4OHT-inducible jejunal enteroids (*VilCreERT2/Hnf4a*^{fx/fx}) were treated with 0.5 μ mol/L 4OHT (Cayman Chemical Company, Ann Arbor, MI) for 24 hours and then split. The jejunal enteroids were harvested on days 2 and 4 after the last passage, and the total RNA was isolated. Induction of differentiation into Paneth-like jejunal enteroids was achieved using a method described previously by Yin et al.³⁴ Briefly, 4OHT-inducible enteroids were split, and CHIR 99021 (3 μ mol/L; Axon Medchem, Reston, VA) and VPA (1 mmol/L; MilliporeSigma, Burlington, MA) were added to the culture medium for 6 days. After 5 days of treatment, 4OHT was added for 24 hours to induce HNF4 α loss. The jejunal enteroids were then passaged, and the culture medium was further supplemented with CHIR (3 μ mol/L) and DAPT (10 μ mol/L; MilliporeSigma). Total RNA was isolated 2 and 4 days after the passage. For *Wnt3* rescue experiments, 200 ng/mL of recombinant mouse *Wnt3A* protein (Abcam, Waltham, MA) was added to the culture medium. The culture media were changed every 3 days, and jejunal enteroids were cultured for 5 days. Live images of enteroids were acquired using a Zeiss Axiovert 200M microscope (Carl Zeiss Canada, Toronto, Canada) or a Zeiss Celldiscoverer 7 instrument. Before the enteroids underwent total RNA isolation, Matrigel domes were dissolved in Cell Recovery Solution (Millipore Sigma).

Co-cultures of Mesenchymal Cells and Enteroids

The primary culture of mesenchymal cells was established as previously described.³⁷ To allow visualization during co-culture, mesenchymal cells were infected with the

pLKO.1-puro-CMV-TurboGFP plasmid (Sigma Aldrich, Saint-Louis, MO). Viruses were produced in 293T cells using the ViraPower Lentiviral Packaging Mix (Invitrogen). The isolation of jejunal crypts to form enteroids was performed as previously described.⁶² After isolating intestinal crypts from *Hnf4a*^{ΔIEC} and control mice, TurboGFP-positive mesenchymal cells were recovered using trypsin-EDTA and enumerated. A total of 10,000 mesenchymal cells per well were mixed gently and seeded. Crypts and mesenchymal cell mixes were then washed to remove any residual trypsin and centrifuged, and the pellet was resuspended in Matrigel. Culture media were added and refreshed every 2–3 days. Photographs were taken every day for 5 days using a Zeiss Celldiscoverer 7.

Co-culture of Sorted Paneth and *Lgr5*⁺ Stem Cells

The co-culture method was adapted from previous studies.^{63,64} Small intestinal crypts from *Hnf4a*^{ΔIEC}, control, and *Lgr5*-EGFP-ires-creERT2 mice were isolated as described above. Single cells were obtained from crypts using TrypLE Express solution (Gibco, Thermo Fisher, Waltham, MA). After dissociation, cells were filtered using a 40- μ m cell strainer, centrifuged, and washed using PBS. Cells were put in FACS buffer (PBS 1% BSA), and suspensions from *Hnf4a*^{ΔIEC} and control mice were labeled using a PE-conjugated anti-CD24 antibody (eBioscience, San Diego, CA). Cells from each condition were then washed 2 times using FACS buffer, resuspended in an appropriate volume of the same buffer, and filtered again using a 40- μ m strainer. Cells were analyzed with BD FACSJazz cell sorter (BD Biosciences). Single cells were gated by forward scatter and side scatter. *Lgr5*-GFP^{Hi} stem cells, *Hnf4a*^{ΔIEC}-CD24^{Hi} Paneth cells, and control CD24^{Hi} Paneth cells were sorted. For 1 well, 2,500 stem cells were mixed with 2,500 control or *Hnf4a*^{ΔIEC} Paneth cells to obtain 2 independent co-cultures. Cells were centrifuged, and pellets were resuspended in 100 μ L/well of enteroids medium containing Y-27632. Suspensions were then seeded in a round bottom ultra-low attachment 96-well plate (Corning, Corning, NY) and left on ice for 15 minutes. The plate was centrifuged at 300g for 5 minutes at 4°C, and 10 μ L of Matrigel (BD Biosciences) was added on top of the cells. Cultures were kept at 37°C for 12 days, and medium was partially changed every 3 days. At day 12, organoids and their ramifications were counted, and areas were measured using ImageJ.

RNA Extraction and Quantitative Real-Time Polymerase Chain Reaction

Total RNA from crypts, jejunal enteroids, or co-cultures was isolated using the RNeasy Mini kit (Qiagen, Hilden, Germany), according to the manufacturer's recommendations.

One microgram of total RNA was used for cDNA synthesis (20 μ L per reaction). The reaction was performed at 50°C for 1 hour with 35 units of Superscript IV Reverse Transcriptase (Invitrogen, Thermo Fisher Scientific), 1 mmol/L dNTPs (Bio Basic, Markham, Canada), and 40 mU oligo(dT)₁₂₋₁₈. cDNA samples were diluted 10-fold before

quantitative polymerase chain reaction analysis was performed. Quantitative real-time polymerase chain reactions (RT-qPCRs) were performed using 2 μ L of diluted cDNA and FastStart Essential DNA Green Master (Roche, Indianapolis, MN). RT-qPCR was performed using a LightCycler 96 system (Roche). Gene expression was normalized relative to the mRNA expression of the TATA-box binding protein (*TBP*).

Protein Extraction and Western Blot Analysis

Total protein extraction from epithelial crypts was performed as previously described.⁶⁵ A BCA protein assay was performed to quantify the proteins. Fresh extracts (35 μ g) were loaded onto a Nupage 4-12% Bis-Tris gel (Invitrogen). Proteins were then transferred onto a polyvinylidene fluoride membrane (Roche), which was blocked in 10% non-fat milk diluted in PBS/0.1% Tween20. To monitor the expression of WNT3, HNF4 α , and actin in the crypt extracts, the following antibodies were used: anti-WNT3 antibody (Abcam; ab32249), anti-HNF4 α antibody C-19 (Santa Cruz Biotechnology, Dallas, TX; SC-6556), and anti-actin antibody clone C4 (MilliporeSigma; MAB1501R). Horseradish peroxidase-linked secondary antibodies were used in combination with ECL-Prime Western blotting Detection Reagent (GE Healthcare, Chicago, IL) to detect the signals.

EdU Incorporation Assays

EdU-incorporation assays were performed to assess proliferation in dimethyl sulfoxide (DMSO)- or 4OHT-treated inducible jejunal enteroids. Imaging and flow cytometry kits (Invitrogen) were used for analysis.

For imaging experiments, enteroids were harvested 4 days after the last passage (see the deletion protocol in *Jejunal Enteroid Culture* section). A Click-iT EdU Cell Proliferation Kit for Imaging (Alexa Fluor 555; Invitrogen) was used according to the manufacturer's recommendations. EdU was incubated with the jejunal enteroids for 60 minutes before fixation. Images were taken using an Olympus FluoView FV1000 confocal microscope (Olympus, Shinjuku, Tokyo, Japan). For flow cytometry experiments, jejunal enteroids were collected 2 and 4 days after passage and mechanically dissociated as single cells. A Click-iT EdU Alexa Fluor 647 Flow Cytometry Assay Kit (Invitrogen) was used according to the manufacturer's recommendations. Cells were analyzed using a Becton Dickinson LSRFortessa flow cytometer (BD Biosciences).

RNA-Seq

Total RNA from inducible jejunal enteroids (DMSO and 4OHT), Wnt3a-treated enteroids (DMSO + Wnt3a and 4OHT + Wnt3a), or co-cultures were isolated as described above. Total RNA was quantified using a NanoDrop Spectrophotometer ND-1000 (NanoDrop Technologies, Thermo Fisher Scientific), and RNA integrity was assessed using a 2100 Bioanalyzer (Agilent Technologies, Santa Clara, CA). Libraries were generated from 250 ng of total RNA as follows: mRNA enrichment was performed using the NEBNext Poly(A) Magnetic Isolation Module (New England BioLabs, Ipswich, MA). cDNA synthesis was achieved using the

NEBNext RNA First Strand Synthesis and NEBNext Ultra Directional RNA Second Strand Synthesis Module (New England BioLabs). The remaining library preparation steps were performed using the NEBNext Ultra II DNA Library Prep Kit for Illumina (New England BioLabs). Adapters and polymerase chain reaction primers were purchased from New England BioLabs. Libraries were quantified using the Quant-iT PicoGreen dsDNA Assay Kit (Life Technologies, Thermo Fisher Scientific) and the Kapa Illumina GA with the Revised Primers-SYBR Fast Universal kit (Kapa Biosystems, MilliporeSigma). Average fragment sizes were determined using a LabChip GX instrument (PerkinElmer). The libraries were normalized, denatured in 0.05 mol/L NaOH, diluted to 200 pmol/L, and neutralized using HT1 buffer. Clustering was performed on an Illumina cBot (Illumina, San Diego, CA), and the flow cell was run on a HiSeq 4000 for 2×100 cycles (paired-end mode) following the manufacturer's instructions. A phiX library was used as a control and was mixed with the libraries at the 1% level. The Illumina control software used was HCS HD 3.4.0.38, and the real-time analysis program was RTA v. 2.7.7. The bcl2fastq v2.20 program was then used to demultiplex samples and generate fastq reads. Cell culture, total RNA extraction, and RNA-seq analysis of HCT116 cells overexpressing HNF4A2 have been described previously.⁴⁵

Immunofluorescence

Paneth cells in DMSO- or 4OHT-treated jejunal enteroids were visualized by lysozyme-targeting immunofluorescence. After *Hnf4a* deletion, enteroids were split, and Matrigel domes were placed on glass coverslips in 24-well plates. Three days after passage, the cells were fixed using 4% paraformaldehyde, directly on Matrigel domes, for 30 minutes. The enteroids were then permeabilized with 0.1% Triton X-100 and blocked with 2% bovine serum albumin. Anti-lysozyme antibody (Agilent Dako) and anti-rabbit Alexa Fluor 488 secondary antibody (Invitrogen) were used to stain the Paneth cells. Nuclei were stained with DAPI, and coverslips were mounted on microscope slides using Thermo Scientific Shandon Immu-Mount (Thermo Fisher). The stained enteroids were visualized using an Olympus Fluoview FV1000 confocal microscope.

Bioinformatics

Bioinformatics analysis of differential gene expression obtained from RNA-seq was performed using the Bioinformatic platform at the University of Sherbrooke, Department of Biochemistry and Functional Genomics. Quality control, pre- and post-trimming was performed with R package fastqcr v0.1.2 (<https://github.com/kassambara/fastqcr>).⁶⁶ Quality and adapter trimming of RNA-seq libraries were performed with Trim Galore version 0.6.4_dev (https://www.bioinformatics.babraham.ac.uk/projects/trim_galore/). Co-cultures raw RNA-seq reads were attributed to the genomes of relevant mouse (version GRCh38) and human (version GRCh38) species using the Sargasso tool (module species_separator rnaseq in a conservative strategy

(<http://statbio.github.io/Sargasso>) and following the bioinformatic procedure from Qiu et al.³⁹ Library normalization and quality control was performed with R package edgeR version 3.34.0,⁶⁷ and differential expression analysis was performed with R package limma v.3.50.1.⁶⁸ In the design matrix, batch effect was accounted because replicates from every condition were coming from 2 different temporal experiments. Genes were retained when their FDR was less than 0.05 and absolute log fold change greater than 1 (just for the co-culture RNA-seq analysis). They were then passed to DAVID version 6.8⁶⁹ for search of enriched GO, which also resulted in a list of GO that passed FDR threshold of 0.05.

Small intestinal epithelial cell lineages were assessed using the GSEA⁷⁰ of signature gene sets previously obtained using plate-based single-cell RNA-sequencing (GEO accession number GSE92332).³³ Gene ontology analysis was performed using ShinyGO V0.76.⁷¹ ChIP-seq analyses of the *Wnt3* gene were performed using the Cistrome Data Browser tool.^{72,73} HNF4A binding sites on the *Wnt3* gene have been identified using ConTra V3.⁷⁴ Venn diagrams were generated using GeneVenn (<http://genevenn.sourceforge.net/>).

Three-Dimensional Imaging of Co-cultures

To preserve the three-dimensional structure of jejunal enteroid-mesenchymal cell interactions, live co-culture imaging was performed. *Hnf4a*^{flx/flx} jejunal enteroids co-cultured with mesenchymal cells were plated in a 60 mm Petri dish to allow the use of a water-dipping Plan-APO-CHROMAT 40x/1.4 objective lens (Zeiss). First, 5-day-old co-cultures were labeled with Hoechst 33342 (Cell Signaling Technology, New England Biolabs) for 15 minutes at 37°C, followed by incubation with CellMask Deep Red Plasma Membrane Stain (Invitrogen) for 10 minutes at 37°C. This staining allowed the visualization of cell membranes. After several washes, the culture medium was replaced in the Petri dish, and Prolong Live Antifade Reagent (Invitrogen) was added and incubated for 1 hour at 37°C to minimize photobleaching during live cell imaging. All images were captured using a Zeiss LSM 880 laser scanning microscope.

Statistical Analysis

Data were analyzed using the GraphPad Prism version 7. For all RT-qPCR and RNA-seq results, statistical analysis was performed using an unpaired Student *t* test with Welch's correction. EdU-positive cell counts determined by flow cytometry were analyzed using the paired Student *t* test. Data were expressed as mean \pm standard deviation, and differences were considered significant at $P < .05$. Bioinformatic statistical analyses were performed using web-based packages and were considered significant at $P < .05$, with FDR $< 5\%$.

References

1. Gehart H, Clevers H. Tales from the crypt: new insights into intestinal stem cells. *Nat Rev Gastroenterol Hepatol* 2019;16:19–34.

2. Durand A, Donahue B, Peignon G, et al. Functional intestinal stem cells after Paneth cell ablation induced by the loss of transcription factor Math1 (Atoh1). *Proc Natl Acad Sci U S A* 2012;109:8965–8970.
3. Kim TH, Escudero S, Shivdasani RA. Intact function of Lgr5 receptor-expressing intestinal stem cells in the absence of Paneth cells. *Proc Natl Acad Sci U S A* 2012; 109:3932–3937.
4. Kabiri Z, Greicius G, Madan B, et al. Stroma provides an intestinal stem cell niche in the absence of epithelial Wnts. *Development* 2014;141:2206–2215.
5. McCarthy N, Manieri E, Storm EE, et al. Distinct mesenchymal cell populations generate the essential intestinal BMP signaling gradient. *Cell Stem Cell* 2020; 26:391–402 e5.
6. Shoshkes-Carmel M, Wang YJ, Wangenstein KJ, et al. Subepithelial telocytes are an important source of Wnts that supports intestinal crypts. *Nature* 2018; 557:242–246.
7. Farin HF, Van Es JH, Clevers H. Redundant sources of Wnt regulate intestinal stem cells and promote formation of Paneth cells. *Gastroenterology* 2012;143:1518–1529 e7.
8. Greicius G, Kabiri Z, Sigmundsson K, et al. PDGFRalpha(+) pericryptal stromal cells are the critical source of Wnts and RSPO3 for murine intestinal stem cells in vivo. *Proc Natl Acad Sci U S A* 2018; 115:E3173–E3181.
9. Kim JE, Fei L, Yin WC, et al. Single cell and genetic analyses reveal conserved populations and signaling mechanisms of gastrointestinal stromal niches. *Nat Commun* 2020;11:334.
10. Stzpourginski I, Nigro G, Jacob JM, et al. CD34+ mesenchymal cells are a major component of the intestinal stem cells niche at homeostasis and after injury. *Proc Natl Acad Sci U S A* 2017;114:E506–E513.
11. Yu S, Tong K, Zhao Y, et al. Paneth cell multipotency induced by Notch activation following injury. *Cell Stem Cell* 2018;23:46–59 e5.
12. Schmitt M, Schewe M, Sacchetti A, et al. Paneth cells respond to inflammation and contribute to tissue regeneration by acquiring stem-like features through SCF/c-Kit signaling. *Cell Rep* 2018; 24:2312–2328 e7.
13. Jones JC, Brindley CD, Elder NH, et al. Cellular plasticity of Defa4(Cre)-expressing Paneth cells in response to Notch activation and intestinal injury. *Cell Mol Gastroenterol Hepatol* 2019;7:533–554.
14. van Es JH, Jay P, Gregorieff A, et al. Wnt signalling induces maturation of Paneth cells in intestinal crypts. *Nat Cell Biol* 2005;7:381–386.
15. Bastide P, Darido C, Pannequin J, et al. Sox9 regulates cell proliferation and is required for Paneth cell differentiation in the intestinal epithelium. *J Cell Biol* 2007; 178:635–648.
16. Mori-Akiyama Y, van den Born M, van Es JH, et al. SOX9 is required for the differentiation of paneth cells in the intestinal epithelium. *Gastroenterology* 2007; 133:539–546.
17. Tanaka T, Jiang S, Hotta H, et al. Dysregulated expression of P1 and P2 promoter-driven hepatocyte nuclear factor-4alpha in the pathogenesis of human cancer. *J Pathol* 2006;208:662–672.
18. Babeu JP, Darsigny M, Lussier CR, et al. Hepatocyte nuclear factor 4alpha contributes to an intestinal epithelial phenotype in vitro and plays a partial role in mouse intestinal epithelium differentiation. *Am J Physiol Gastrointest Liver Physiol* 2009;297:G124–G134.
19. Parviz F, Matullo C, Garrison WD, et al. Hepatocyte nuclear factor 4alpha controls the development of a hepatic epithelium and liver morphogenesis. *Nat Genet* 2003; 34:292–296.
20. Spath GF, Weiss MC. Hepatocyte nuclear factor 4 provokes expression of epithelial marker genes, acting as a morphogen in dedifferentiated hepatoma cells. *J Cell Biol* 1998;140:935–946.
21. Verzi MP, Shin H, San Roman AK, et al. Intestinal master transcription factor CDX2 controls chromatin access for partner transcription factor binding. *Mol Cell Biol* 2013; 33:281–292.
22. San Roman AK, Aronson BE, Krasinski SD, et al. Transcription factors GATA4 and HNF4A control distinct aspects of intestinal homeostasis in conjunction with transcription factor CDX2. *J Biol Chem* 2015; 290:1850–1860.
23. Chen L, Toke NH, Luo S, et al. A reinforcing HNF4-SMAD4 feed-forward module stabilizes enterocyte identity. *Nat Genet* 2019;51:777–785.
24. Chen L, Vasoya RP, Toke NH, et al. HNF4 regulates fatty acid oxidation and is required for renewal of intestinal stem cells in mice. *Gastroenterology* 2020;158:985–999 e9.
25. Darsigny M, Babeu JP, Seidman EG, et al. Hepatocyte nuclear factor-4alpha promotes gut neoplasia in mice and protects against the production of reactive oxygen species. *Cancer Res* 2010;70:9423–9433.
26. Barker N, Ridgway RA, van Es JH, et al. Crypt stem cells as the cells-of-origin of intestinal cancer. *Nature* 2009; 457:608–611.
27. Consortium UIG, Barrett JC, Lee JC, et al. Genome-wide association study of ulcerative colitis identifies three new susceptibility loci, including the HNF4A region. *Nat Genet* 2009;41:1330–1334.
28. Jostins L, Ripke S, Weersma RK, et al. Host-microbe interactions have shaped the genetic architecture of inflammatory bowel disease. *Nature* 2012;491:119–124.
29. Darsigny M, Babeu JP, Dupuis AA, et al. Loss of hepatocyte-nuclear-factor-4alpha affects colonic ion transport and causes chronic inflammation resembling inflammatory bowel disease in mice. *PLoS One* 2009;4: e7609.
30. Montenegro-Miranda PS, van der Meer JHM, Jones C, et al. A novel organoid model of damage and repair identifies HNF4alpha as a critical regulator of intestinal epithelial regeneration. *Cell Mol Gastroenterol Hepatol* 2020.
31. Kim TH, Li F, Ferreiro-Neira I, et al. Broadly permissive intestinal chromatin underlies lateral inhibition and cell plasticity. *Nature* 2014;506:511–515.

32. Gehart H, van Es JH, Hamer K, et al. Identification of enteroendocrine regulators by real-time single-cell differentiation mapping. *Cell* 2019;176:1158–1173 e16.
33. Haber AL, Biton M, Rogel N, et al. A single-cell survey of the small intestinal epithelium. *Nature* 2017;551:333–339.
34. Yin X, Farin HF, van Es JH, et al. Niche-independent high-purity cultures of Lgr5+ intestinal stem cells and their progeny. *Nat Methods* 2014;11:106–112.
35. Farin HF, Jordens I, Mosa MH, et al. Visualization of a short-range Wnt gradient in the intestinal stem-cell niche. *Nature* 2016;530:340–343.
36. Young MA, Daly CS, Taylor E, et al. Subtle deregulation of the Wnt-signaling pathway through loss of Apc2 reduces the fitness of intestinal stem cells. *Stem Cells* 2018;36:114–122.
37. Lussier CR, Babeu JP, Auclair BA, et al. Hepatocyte nuclear factor-4alpha promotes differentiation of intestinal epithelial cells in a coculture system. *Am J Physiol Gastrointest Liver Physiol* 2008;294:G418–G428.
38. Cretoiu D, Cretoiu SM, Simionescu AA, et al. Telocytes, a distinct type of cell among the stromal cells present in the lamina propria of jejunum. *Histol Histopathol* 2012;27:1067–1078.
39. Qiu J, Dando O, Baxter PS, et al. Mixed-species RNA-seq for elucidation of non-cell-autonomous control of gene transcription. *Nat Protoc* 2018;13:2176–2199.
40. McCarthy N, Kraiczky J, Shivdasani RA. Cellular and molecular architecture of the intestinal stem cell niche. *Nat Cell Biol* 2020;22:1033–1041.
41. Cattin AL, Le Beyec J, Barreau F, et al. Hepatocyte nuclear factor 4alpha, a key factor for homeostasis, cell architecture, and barrier function of the adult intestinal epithelium. *Mol Cell Biol* 2009;29:6294–6308.
42. Vuong LM, Chellappa K, Dhahbi JM, et al. Differential effects of hepatocyte nuclear factor 4alpha isoforms on tumor growth and T-cell factor 4/AP-1 interactions in human colorectal cancer cells. *Mol Cell Biol* 2015;35:3471–3490.
43. Consortium EP. An integrated encyclopedia of DNA elements in the human genome. *Nature* 2012;489:57–74.
44. Davison JM, Lickwar CR, Song L, et al. Microbiota regulate intestinal epithelial gene expression by suppressing the transcription factor hepatocyte nuclear factor 4 alpha. *Genome Res* 2017;27:1195–1206.
45. Lambert E, Babeu JP, Simoneau J, et al. Human hepatocyte nuclear factor 4-alpha encodes isoforms with distinct transcriptional functions. *Mol Cell Proteomics* 2020;19:808–827.
46. Bankaitis ED, Ha A, Kuo CJ, et al. Reserve stem cells in intestinal homeostasis and injury. *Gastroenterology* 2018;155:1348–1361.
47. de Sousa EMF, de Sauvage FJ. Cellular plasticity in intestinal homeostasis and disease. *Cell Stem Cell* 2019;24:54–64.
48. Chahar S, Gandhi V, Yu S, et al. Chromatin profiling reveals regulatory network shifts and a protective role for hepatocyte nuclear factor 4alpha during colitis. *Mol Cell Biol* 2014;34:3291–3304.
49. Girard R, Tremblay S, Noll C, et al. The transcription factor hepatocyte nuclear factor 4A acts in the intestine to promote white adipose tissue energy storage. *Nat Commun* 2022;13:224.
50. Adolph TE, Tomczak MF, Niederreiter L, et al. Paneth cells as a site of origin for intestinal inflammation. *Nature* 2013;503:272–276.
51. Karin M, Clevers H. Reparative inflammation takes charge of tissue regeneration. *Nature* 2016;529:307–315.
52. Vermeulen L, De Sousa EMF, van der Heijden M, et al. Wnt activity defines colon cancer stem cells and is regulated by the microenvironment. *Nat Cell Biol* 2010;12:468–476.
53. Zhang B, Wang J, Wang X, et al. Proteogenomic characterization of human colon and rectal cancer. *Nature* 2014;513:382–387.
54. Chen L, Toke NH, Luo S, et al. HNF4 factors control chromatin accessibility and are redundantly required for maturation of the fetal intestine. *Development* 2019:146.
55. Bian J, Dannappel M, Wan C, et al. Transcriptional regulation of Wnt/beta-catenin pathway in colorectal cancer. *Cells* 2020;9.
56. Gougelet A, Torre C, Veber P, et al. T-cell factor 4 and beta-catenin chromatin occupancies pattern zonal liver metabolism in mice. *Hepatology* 2014;59:2344–2357.
57. Babeu JP, Jones C, Geha S, et al. P1 promoter-driven HNF4alpha isoforms are specifically repressed by beta-catenin signaling in colorectal cancer cells. *J Cell Sci* 2018;131.
58. Vogg MC, Beccari L, Iglesias Olle L, et al. An evolutionarily-conserved Wnt3/beta-catenin/Sp5 feedback loop restricts head organizer activity in Hydra. *Nat Commun* 2019;10:312.
59. van Es JH, Wiebrands K, Lopez-Iglesias C, et al. Enterendocrine and tuft cells support Lgr5 stem cells on Paneth cell depletion. *Proc Natl Acad Sci U S A* 2019.
60. Madison BB, Dunbar L, Qiao XT, et al. Cis elements of the villin gene control expression in restricted domains of the vertical (crypt) and horizontal (duodenum, cecum) axes of the intestine. *J Biol Chem* 2002;277:33275–33283.
61. el Marjou F, Janssen KP, Chang BH, et al. Tissue-specific and inducible Cre-mediated recombination in the gut epithelium. *Genesis* 2004;39:186–193.
62. Gonneaud A, Jones C, Turgeon N, et al. A SILAC-based method for quantitative proteomic analysis of intestinal organoids. *Sci Rep* 2016;6:38195.
63. Sato T, van Es JH, Snippert HJ, et al. Paneth cells constitute the niche for Lgr5 stem cells in intestinal crypts. *Nature* 2011;469:415–418.
64. Yilmaz OH, Katajisto P, Lamming DW, et al. mTORC1 in the Paneth cell niche couples intestinal stem-cell function to calorie intake. *Nature* 2012;486:490–495.
65. Boudreau F, Lussier CR, Mongrain S, et al. Loss of cathepsin L activity promotes claudin-1 overexpression and intestinal neoplasia. *FASEB J* 2007;21:3853–3865.
66. Liao Y, Smyth GK, Shi W. The R package Rsubread is easier, faster, cheaper and better for alignment and quantification of RNA sequencing reads. *Nucleic Acids Res* 2019;47:e47.
67. Robinson MD, McCarthy DJ, Smyth GK. edgeR: a Bioconductor package for differential expression analysis of

- digital gene expression data. *Bioinformatics* 2010; 26:139–140.
68. Ritchie ME, Phipson B, Wu D, et al. limma powers differential expression analyses for RNA-sequencing and microarray studies. *Nucleic Acids Res* 2015;43:e47.
 69. Jiao X, Sherman BT, Huang da W, et al. DAVID-WS: a stateful web service to facilitate gene/protein list analysis. *Bioinformatics* 2012;28:1805–1806.
 70. Subramanian A, Tamayo P, Mootha VK, et al. Gene set enrichment analysis: a knowledge-based approach for interpreting genome-wide expression profiles. *Proc Natl Acad Sci U S A* 2005;102:15545–15550.
 71. Ge SX, Jung D, Yao R. ShinyGO: a graphical gene-set enrichment tool for animals and plants. *Bioinformatics* 2020;36:2628–2629.
 72. Mei S, Qin Q, Wu Q, et al. Cistrome Data Browser: a data portal for ChIP-Seq and chromatin accessibility data in human and mouse. *Nucleic Acids Res* 2017; 45(D1):D658–D662.
 73. Zheng R, Wan C, Mei S, et al. Cistrome Data Browser: expanded datasets and new tools for gene regulatory analysis. *Nucleic Acids Res* 2019; 47(D1):D729–D735.
 74. Kreft L, Soete A, Hulpiau P, et al. ConTra v3: a tool to identify transcription factor binding sites across species, update 2017. *Nucleic Acids Res* 2017;45(W1): W490–W494.

Received April 26, 2021. Accepted November 28, 2022.

Correspondence

Address correspondence to: Francois Boudreau, PhD, Department of Immunology and Cell Biology, Université de Sherbrooke, 3201 Rue Jean-Mignault, Sherbrooke, Québec, J1E 4K8 Canada. e-mail: Francois.Boudreau@USherbrooke.ca.

Acknowledgments

The authors thank the McGill University and Génome Québec Innovation Center for RNA-Seq services.

CRedit Authorship Contributions

Christine Jones, MSc (Conceptualization: Equal; Data curation: Equal; Formal analysis: Equal; Investigation: Equal; Methodology: Equal; Validation: Lead; Writing – original draft: Supporting; Writing – review & editing: Supporting)

Mariano Avino, PhD (Data curation: Equal; Formal analysis: Equal; Methodology: Equal; Software: Lead; Writing – review & editing: Supporting)

Veronique Giroux (Conceptualization: Supporting; Formal analysis: Supporting; Methodology: Supporting; Resources: Supporting; Supervision: Supporting)

Francois Boudreau (Conceptualization: Equal; Formal analysis: Equal; Funding acquisition: Lead; Investigation: Equal; Methodology: Equal; Project administration: Equal; Resources: Lead; Supervision: Lead; Writing – original draft: Lead; Writing – review & editing: Lead)

Conflicts of interest

The authors disclose no conflicts.

Funding

Supported by the Canadian Institutes of Health Research (PJT-156180 and PJT-183704) and the Natural Sciences and Engineering Research Council of Canada (RGPIN-2017-06096). F.B. and V.G. are members of the FRQS-funded “Centre de recherche du CHUS” (CR-CHUS). V.G. is the recipient of the Canada Research Chair in Gastrointestinal Stem Cell Biology.